REPORT 1209

DEVELOPMENT OF TURBULENCE-MEASURING EQUIPMENT [1]

By Leslie S. G. Kovásznay

SUMMARY

Hot-wire turbulence-measuring equipment has been developed to meet the more stringent requirements involved in the measurement of fluctuations in flow parameters at supersonic velocities. The higher mean speed necessitates the resolution of higher frequency components than at low speed, and the relatively low turbulence level present at supersonic speed makes necessary an improved noise level for the equipment. The equipment covers the frequency range from 2 to about 70,000 cycles per second. Constant-current operation is employed. Compensation for hot-wire lag is adjusted manually using square-wave testing to indicate proper setting. These and other features make the equipment adaptable to all-purpose turbulence work with improved utility and accuracy over that of older types of equipment. Sample measurements are given to demonstrate the performance.

INTRODUCTION

The hot-wire technique at low subsonic speeds has become a standard tool of turbulence research. When high-speed and supersonic wind tunnels appeared, the interest was focused more on the effects of compressibility than viscosity. This led to the accumulation of a wealth of data on supersonic flow devoid of quantitative measurements relating to the effects of the viscosity and, in particular, with respect to the properties of the turbulence that was present.

The natural development calls for information on turbulence in supersonic wind tunnels just as it was needed in the case of low-speed wind tunnels in the last decade.

The feasibility of using hot-wires in a supersonic flow was first demonstrated by Dryden and Schubauer in 1946, when they operated a 0.0003-inch-diameter tungsten wire in the Aberdeen wind tunnel and observed fluctuations with it. (This work is unpublished.) This type of measurement was repeated in the Langley 9-inch supersonic tunnel at Langley Field in late 1947.

It became apparent, after a closer examination of the problem, that there were three major problems to be solved before actual turbulence measurements could be obtained in supersonic flow:

(1) To extend the response of the hot-wire probe and its associated equipment to much higher frequencies

(2) To determine the heat-loss law of the hot-wire in compressible flow, thus replacing the well-established King's law, valid only for incompressible flow

(3) To interpret the measurements obtained in a compressible flow, where there are three parameters of the flow instead of the velocity alone, as in the low-speed case of turbulence

The attack on these problems was conducted in separate phases. The development of hot-wire equipment capable of handling signals up to 50 to 70 kilocycles with a tolerable noise level is presented in this report. The work on the determination of the laws of heat loss from wires and wire sensitivity in supersonic flow was conducted at The Johns Hopkins University and reported in references 1 and 2. The analytical decomposition of the fluctuating flow field into three modes and the interpretation of turbulence measurements in a supersonic wind tunnel are given in reference 3.

After the equipment was put into operation and was used to measure turbulence in supersonic flow, some modifications in the equipment became desirable. Complete new units have been built that have incorporated these improvements. In the text and figures, the term "original" will be used when referring to the equipment completed in the Bureau of Standards in 1951 and the term "new," when the equipment presently in operation at The Johns Hopkins University is mentioned.

The original equipment was developed as a project conducted under the sponsorship and with the financial assistance of the National Advisory Committee for Aeronautics. The work was carried on in the Electronics Division, Engineering Electronics Section, of the National Bureau of Standards and was one phase of a joint project undertaken by NBS under the sponsorship of the NACA and by The Johns Hopkins University under the sponsorship of the Bureau of Ordnance of the U. S. Navy Department. By informal arrangement, the author, who is associated with The Johns Hopkins University, spent part time in the NBS laboratory directing the design and construction. The author wishes to express his thanks to Dr. H. L. Dryden, who originated the cooperative arrangement between NBS and The Johns Hopkins University, and to Dr. G. B. Schubauer, who assisted in putting it into effect and promoted the work by his support and interest. The author is much indebted to Mr. Merlin Davis who did most of the detail design and experimental work. In addition, his conscientious help with the compilation and assembly of the report material was invaluable. Thanks are due to Mr. J. G. Reid,

[1] This investigation was conducted at the National Bureau of Standards and the results were originally presented in NACA TN 2839, "Development of Turbulence-Measuring Equipment" by Leslie S. G. Kovásznay, which was released in 1953. This Technical Note has been revised and is superseded by the present paper.

Jr., for supervision of the work as well as for his many valuable suggestions, such as the use of the biased-diode system of square-law detection, and to Mr. H. H. Parnell who helped with procurement and shop problems.

The modifications were later developed by the author at The Johns Hopkins University as a part of the turbulence research program jointly sponsored by the U. S. Navy, Bureau of Ordnance, and Project Squid. The author is indebted to Mr. Victor Svec, whose help was essential in this latter phase of the program. Thanks are also due to the Ballistic Research Laboratory of Aberdeen Proving Ground for giving supersonic-wind-tunnel time for first testing this equipment in supersonic flow.

SYMBOLS

A, B, C	nondimensional constants of supersonic hot-wire heat loss
A', B'	convection constant, cm-g-sec
a, b	arbitrary random functions of time with zero time average
a_e	dimensionless overheating ratio, $\frac{R_e-R_f}{R_f}$
a_w	dimensionless overheating ratio, $\frac{R_w-R_f}{R_f}$
a_w'	dimensionless overheating ratio, $\frac{R_w-R_e}{R_e}$
C_T	thermal capacity of wire, ergs/°C
d	diameter of wire, in. in figure 7, cm elsewhere
E	thermal energy accumulated in wire, ergs
e	voltage, v
e_v	voltage signal that would be attained without thermal lag, v
e_0	characteristic voltage of wire, $2R_fI_0$
e'	input voltage to diode circuit, v, $e-IR_m$
$\bar{e}$	mean voltage drop across wire, v
Δe	voltage fluctuation, v
Δe_m	voltage fluctuation caused by 1-percent mass-flow fluctuation, v
Δe_T	voltage fluctuation caused by 1-percent temperature fluctuation, v
Δe_v	virtual voltage fluctuation that would be produced in absence of thermal lag, v
Δe_1	voltage fluctuation produced by 1-percent velocity fluctuation, v
f	frequency, cps
f_{max}	maximum frequency, cps
$g=\alpha T_o$	
g_m	tube transconductance, mhos
H	heat loss of wire per unit time, ergs/sec
I	heating current, amp
I_0	characteristic current of wire necessary to attain $a_w'=1$ at $U=0$, amp
i	imaginary unit, $\sqrt{-1}$
k_o	heat conductivity of air at stagnation temperature, ergs/cm/sec/°C
L	self-inductance, h
l	hot-wire length, cm
l_x	resolution length, cm
M	time constant of thermal lag in hot-wire, sec
M_o	time constant of wire when operated unheated (resistance thermometer), sec
m'	percent mass-flow fluctuation, $100\frac{\sqrt{\overline{\Delta(\rho U)^2}}}{\bar{\rho}\bar{U}}$
Nu	Nusselt number
Nu_o	Nusselt number at stagnation temperature
n	thermal lag constant of a particular wire, amp² sec
R	resistance of wire, ohms
R_{ab}	correlation coefficient, $\frac{\overline{ab}}{\sqrt{\overline{a^2}}\sqrt{\overline{b^2}}}$
R_e	resistance of wire at temperature T_e, ohms
Re	Reynolds number
Re_0	characteristic Reynolds number of wire
R_f	resistance of wire at reference temperature T_f, ohms
R_m	meter resistance in square detector, ohms
R_{mT}	mass-flow-temperature correlation
R_w	resistance of wire at temperature T_w, ohms
r	ratio of mean-square sum and difference, ∇/Σ
T	temperature absolute, °K
T_e	equilibrium temperature attained if wire is unheated, °K
T_f	reference temperature (usually 273° K), °K
T_o	stagnation temperature, °K
ΔT_o	stagnation temperature fluctuation, °K
T_w	wire temperature when heated, °K
t	time, sec
U	mean velocity, ft/sec in figure 1, cm/sec elsewhere
ΔU	velocity fluctuation, cm/sec
U_0	characteristic velocity of wire, cm/sec
ΔV	bias voltage step, v
W	heat input of wire, ergs/sec
x	space coordinate parallel to mean-flow direction
y, z	nondimensional parameters depending on hot-wire Reynolds number
α	temperature coefficient of resistivity defined at T_f, 1 per °C
β	deflection of ratiometer needle
η	equilibrium temperature ratio, T_e/T_o
ϑ	percent stagnation-temperature fluctuation, $100\frac{\sqrt{\overline{(\Delta T_o)^2}}}{T_o}$
μ	amplification factor
μ_o	viscosity at stagnation temperature, poises
ξ	ratio of root-mean-square values of two signals
ρ	density, g/cm³
$\Delta\rho$	density fluctuation, g/cm³
Σ	mean square of sum of two signals, $\overline{(a+b)^2}$
τ	temperature loading, $\frac{T_w-T_e}{T_o}$
ϕ, C'	nondimensional parameters depending on operating conditions of wire
∇	mean square of difference of two signals, $\overline{(a-b)^2}$
$\overline{(\,)}$	time average

GENERAL REMARKS ON HOT-WIRE METHOD

The hot-wire method for measuring turbulent fluctuations of the flow parameters essentially relies on the law of heat loss from a fine wire located in an air stream.

For the usual condition, when the mean flow is large compared with the turbulent velocity fluctuations, the whole turbulent pattern is swept by the wire and, as a first approximation, one can assume that the time history recorded by a stationary hot-wire probe is really a record of the moving turbulence pattern along the space coordinate x parallel to the mean-flow direction. Similarly the long-range behavior of the turbulent pattern in time is identified with the change in conditions downstream along the coordinate x. This interchange of space and time coordinates becomes justified, in the limit, as the turbulent velocity vanishes compared with the mean flow. This approximation enables one to estimate the resolution in space from the frequency response of the equipment. The hot-wire has two rather important limitations. One is the nonlinearity with velocity; the other is the finite resolution in time and, consequently, in space.

Since heat loss is not a linear function of velocity, it is rather impractical to measure turbulence with zero mean motion. No distinction between the positive and negative values of the velocity is possible because the wire responds only to the absolute magnitude of the velocity. As a result of this situation, the hot-wire is used almost exclusively in flows where there is a substantial mean flow and the turbulent fluctuations and the sensitivity coefficients will depend only on the mean operating conditions.

The resolution length in the direction of the wire is the wire length itself, and its effect on measuring space characteristics (correlation and spectra) is given in references 4, 5, and 6. The resolution length in the flow direction is governed primarily by the frequency response of the system. Define $l_x=\frac{U}{2f_{max}}$ where f_{max} is the maximum frequency of the amplifier, that is, where there is no substantial loss of response, and U is the mean speed of air flow. Figure 1 shows the quantitative relationships. The "resolving power" can be represented by an area having as sides the length of the wire and the resolution length l_x in the direction of flow. The resolution length in the third dimension is negligible, compared with the two lengths mentioned before, because it is governed only by wire diameter, which is always small compared with the length.

The thermal lag of the wire is large enough to make the unaided wire impractical, even for measuring turbulence at low speed. The real advantage of the hot-wire method, however, is not so much its small time lag but the fact that the lag obeys a simple law; therefore approximate compensation can be applied satisfactorily. For higher frequencies the response of the hot-wire falls off inversely proportional to the frequency. If compensation can be achieved up to a factor of 100 (40 decibels), this will extend the useful frequency range by the same factor. If the useful band is assumed as extending up to the "3-decibel point" (approximately 70-percent response in voltage), then the new frequency limit with such a compensation is as follows:

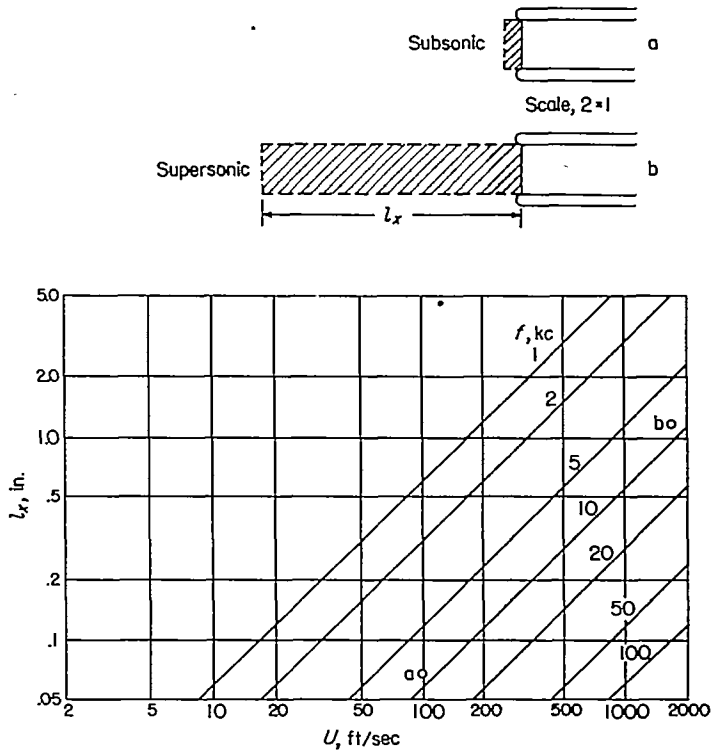

FIGURE 1.—Resolution length of hot-wire anemometer at various speeds.

M, milliseconds	1.6	1.0	0.8	0.4	0.2
f_{max} kc/sec	10	16	20	40	80

The use of fine wires, and consequently low time-constant values, permits higher frequencies but introduces serious mechanical difficulties. Any other turbulence-measuring technique which might be suggested in place of the hot-wire must offer a better resolving power without loss in absolute sensitivity if it is to be an improvement over the hot-wire.

The sensitivity of the hot-wire probe to fluctuations can be derived from the law of heat loss from wires. The wire responds to fluctuations in the heating and cooling conditions imposed by the electric circuit and by the air flow. The static and dynamic equations applying to hot-wire performance in the case of an incompressible-flow medium will be derived as a basis for the design of the equipment, particularly in regard to the choice of the hot-wire thermal-lag compensation system.

The preliminary experiments with hot-wires in supersonic flow (refs. 1 and 2) have proven that the heat-loss functions are not substantially different from those in incompressible flow, nor is there any difference in the order of magnitude. This being the case, the well-established results for incompressible flow can serve as a guide in determining orders of magnitude. In fact, this was the procedure followed to find the design requirements for the development of the present equipment, since systematic data on wires in supersonic flow were available only in the latter phase of the work.

The following formula derived by King (ref. 7) represents the heat loss in incompressible flow for a wire of small diameter:

$$H=l(T_w-T_e)\ (A'\sqrt{U}+B') \tag{1}$$

Using wire resistances R_w and R_e corresponding to T_w and T_e, a useful temperature factor may be defined as follows:

$$a_w'=\frac{R_w-R_e}{R_e}$$

Since α, the temperature coefficient of resistivity, is defined in terms of a reference temperature R_f by

$$R_w=R_f[1+\alpha(T_w-T_f)] \tag{2}$$

other useful temperature factors are:

$$a_w=\frac{R_w-R_f}{R_f}$$

and

$$a_e=\frac{R_e-R_f}{R_f}$$

These become important in temperature measurements.

The conservation of energy requires that the difference between heat generated in the wire and heat lost to the air be equal to the thermal energy accumulated in the wire, so

$$I^2R_w-l(T_w-T_e)(A'\sqrt{U}+B')=C_T\frac{dT_w}{dt} \tag{3}$$

where C_T is the thermal capacity of the wire:

$$C_T=\frac{dE}{dT_w}$$

If the mass of the hot-wire is small and the fluctuations are slow, the right-hand side of equation (3) can be neglected and a quasi-equilibrium equation of state obtained:

$$I^2R_w=l(T_w-T_e)\ (A'\sqrt{U}+B') \tag{3a}$$

For convenience, equation (3a) can be transformed into a nondimensional representation

$$\frac{I^2}{I_0^2}=\frac{2a_w'}{1+a_w'}\left(\sqrt{\frac{U}{U_0}}+1\right) \tag{4}$$

where

$$I_0=\sqrt{\frac{lB'}{2R_f\alpha}}$$

and

$$U_0=\frac{(B')^2}{(A')^2}$$

The new constants R_f, I_0, and U_0 are characteristics of any given wire and have the dimensions of electric current and of velocity in addition to the temperature factor previously mentioned. Equation (4) is formulated in terms of the three fundamental hot-wire variables U, I, and a_w'. Their functional relationship is shown in figure 2. Keeping one variable constant, the usual hot-wire characteristics are obtained as orthogonal sections.

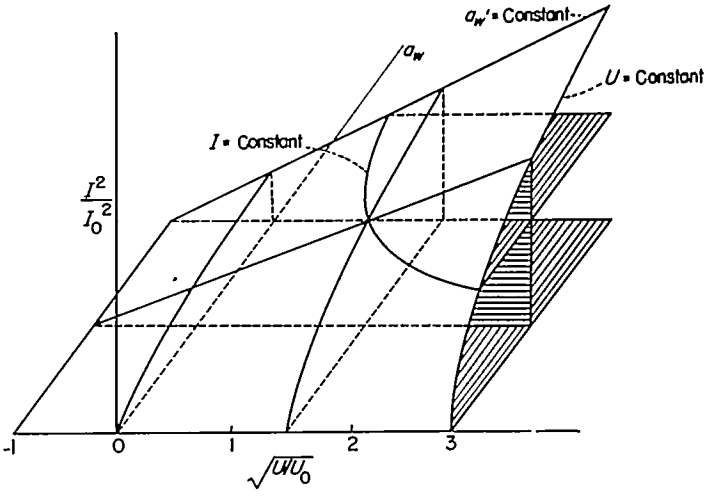

FIGURE 2.—Hot-wire in thermal equilibrium. $a_w'=\frac{R_w-R_e}{R_e}$.

At constant temperature a_w'=Constant the square of the heating current is a linear function of the square root of the velocity. At constant current I=Constant the temperature factor a_w' decreases with increasing velocity. At constant velocity U=Constant the temperature increases faster than linearly with increasing heating current.

The hot-wire, operated in an electrical circuit which provides it with a constant heating current, responds to the velocity fluctuations by temperature fluctuations. These temperature fluctuations are recorded as voltage fluctuations. The value of voltage fluctuations at constant current is

$$\frac{\Delta e}{\bar{e}}=-\frac{a_w'}{2}\frac{1}{1+\sqrt{\frac{U_0}{\bar{U}}}}\frac{\Delta U}{\bar{U}} \tag{5}$$

where Δe stands for the voltage fluctuations (departure from the mean), $\bar{e}=IR_w$ is the mean direct-current voltage drop across the wire, and ΔU is the velocity fluctuation. The negative sign indicates that the wire responds with a voltage decrement to a velocity increment. A nondimensional form of voltage-fluctuation sensitivity valid for all wires at zero Mach number is

$$\frac{\Delta e_1}{e_0}=f\left(\frac{I}{I_0},\ a_w',\ \frac{\bar{U}}{U_0}\right) \tag{6}$$

with $e_0=2R_fI_0$ as a characteristic voltage and Δe_1 as the voltage fluctuation caused by 1-percent velocity fluctuations. The plot is given in figure 3 and indicates that the sensitivity increases with both increasing velocity ratio and increasing mean wire temperature. The results thus obtained are valid only for slow fluctuations because the right-hand side of equation (3) was neglected. For faster fluctuations the thermal lag becomes appreciable. Detailed analysis shows that, within the reach of the linearized theory of fluctuation response, the thermal lag obeys a simple law

$$\Delta e+M\frac{d\Delta e}{dt}=\Delta e_s \tag{7}$$

where Δe_s is the voltage fluctuation that would have been

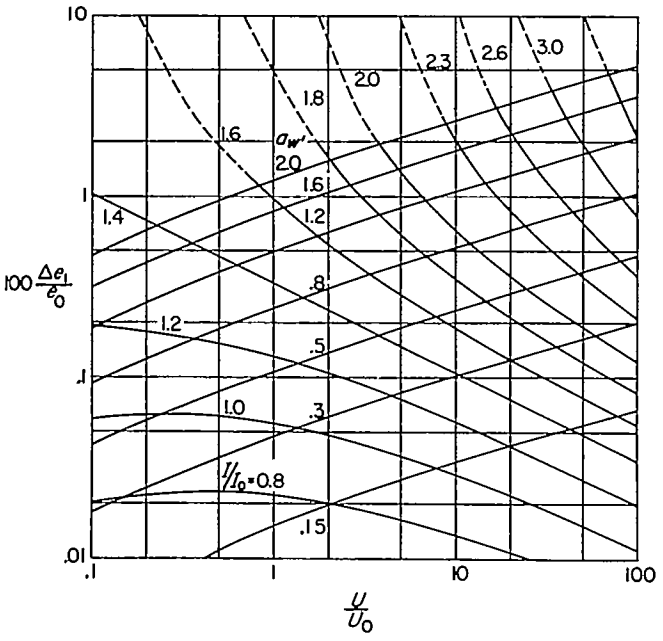

FIGURE 3.—Nondimensional hot-wire sensitivity in low-speed flow

obtained in a thermal quasi equilibrium (eq. (3a) or (5)) and M is the time constant, depending on the operating conditions. The time constant is, in general,

$$M=\frac{C_T}{\left(\frac{\partial H}{\partial T_w}\right)-\left(\frac{\partial W}{\partial T_w}\right)} \quad (8)$$

where C_T is the heat capacity of the wire. With King's law and linear dependence of the resistance on the temperature

$$M=n\frac{a_w'}{I^2} \quad (9)$$

where n is a constant depending upon the properties of the wire. For constant velocity, it will be noted that I^2 becomes a unique function of a_w', for the time constant is then simply proportional to the wire resistance. Where M_0 is the extrapolated value for an unheated wire ($a_w'\to 0$),

$$M=M_0(1+a_w') \quad (10)$$

(This value applies if the wire is used as a resistance thermometer to pick up temperature fluctuations.) The hot-wire thus has four calibration constants: R_f, U_0, I_0, and n. Orders of magnitude for practical hot-wire probes constructed of platinum and tungsten wires varying in diameter from 0.00005 to 0.0003 inch are as follows: R_f, 5 to 50 ohms; U_0, 200 to 300 centimeters per second; I_0, 25 to 150 milliamperes; and n, 10^{-4} to 10^{-6} square amperes times seconds.

The thermal-lag effect (eq. (7)) can be determined for sine waves, and it can be easily shown that the equivalent circuit is a passive four-pole network with a time constant M. The transfer function is complex,

$$\frac{\Delta e}{\Delta e_v}=\frac{1}{1+2\pi i f M} \quad (11)$$

where Δe_v is the signal of virtual voltage fluctuation proportional to the velocity fluctuation and Δe is the actual voltage

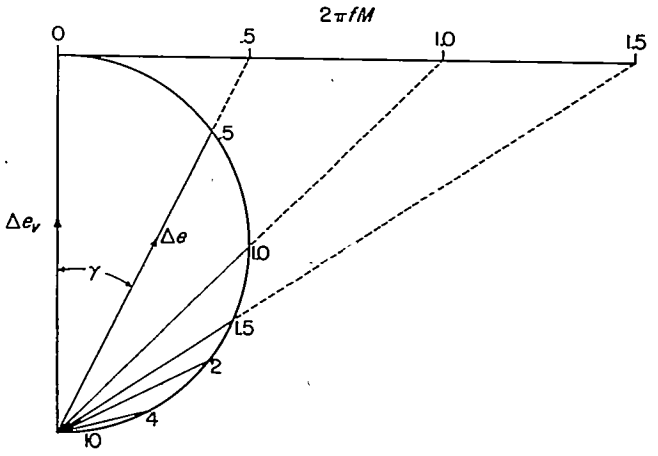

FIGURE 4.—Vector diagram of hot-wire thermal lag. $\left|\frac{\Delta e}{\Delta e_v}\right|=\frac{1}{\sqrt{1+(2\pi fM)^2}}$; $\gamma=\tan^{-1}2\pi fM$.

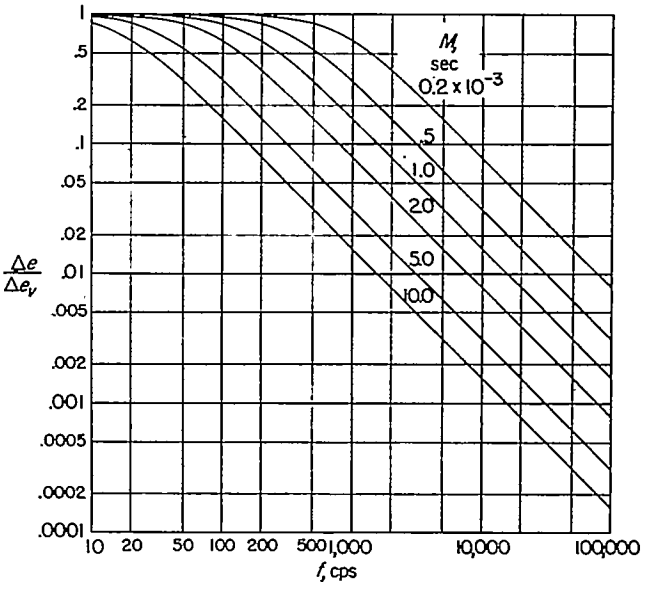

FIGURE 5.—Frequency response of uncompensated hot-wire.

fluctuation. The vector diagram is given in figure 4 and shows both the amplitude reduction and phase lag:

$$\frac{\Delta e}{\Delta e_v}=\frac{\exp\left[-i\tan^{-1}(2\pi fM)\right]}{\sqrt{1+(2\pi fM)^2}} \quad (12)$$

The amplitude reduction for the usual range of time constants is given in figure 5. This figure clearly indicates that the hot-wire anemometer cannot be used for measuring rapid fluctuations unless the thermal-lag effect is substantially reduced by some compensating system. This was first successfully achieved by Dryden and Kuethe (ref. 8). Since then a number of other systems have been devised for reducing thermal-lag effects. These will be discussed more in detail later.

The heat loss at supersonic velocities has been determined experimentally and data are given in references 1 and 2. The fluctuation sensitivities have been determined by logarithmic differentiation. Experiments for a complete range of Mach numbers have been carried out by Lowell (ref. 9) on wires of a large diameter (0.003 inch), but his main attention was focused more on the measurement of

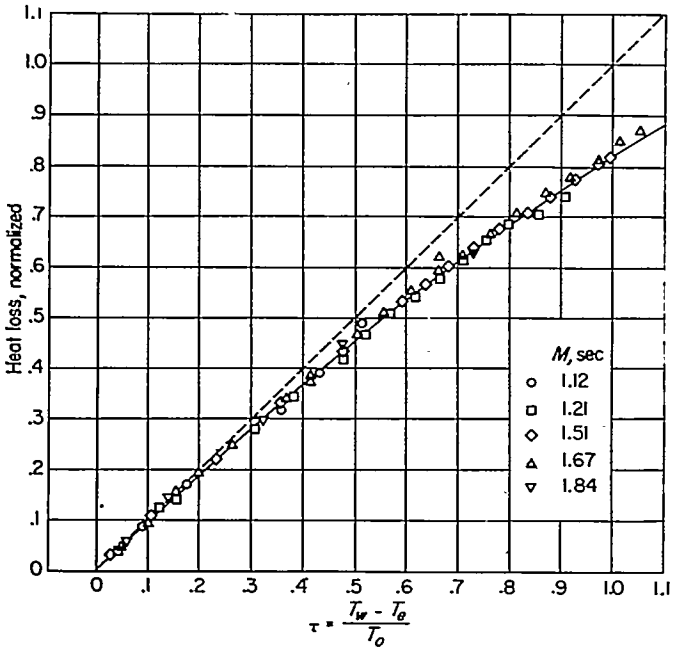

FIGURE 6.—Heat loss of hot-wire as function of wire temperature in supersonic flow.

mean-flow parameter values than on turbulent fluctuations. Recently the heat-loss parameters were remeasured and some new findings are reported by Spangenberg in reference 10.

The results of the experiments conducted in supersonic flow can be summarized as follows: The unheated wire, when exposed to a supersonic air stream, reaches an equilibrium temperature between 93 and 98 percent of the stagnation temperature:

$$\left.\begin{aligned} &\frac{T_e}{T_o}=\eta \\ &\eta \approx 0.93 \text{ to } 0.98 \end{aligned}\right\} \tag{13}$$

The variation of η with Mach number is available from experimental data. If the wire is heated to a temperature T_w, the heat loss is proportional to T_w-T_e as a first approximation. For higher temperatures there is a substantial nonlinear effect. This nonlinear effect does not seem to depend much on the Mach number. Figure 6 shows this variation as a function of temperature loading.

The variation of heat loss on flow parameters can be represented nondimensionally with the Nusselt number as a function of Reynolds number and Mach number. If an appropriate combination of flow parameters is used to form the Reynolds number, the dependence on the Mach number disappears and the Nusselt number becomes a linear function of the square root of the Reynolds number:

$$Nu=\frac{H}{\pi l k_o(T_w-T_e)}=\left(A\sqrt{\frac{\overline{U}\rho d}{\mu_o}}-B\right)(1-C_T) \tag{14}$$

Values of $A=0.58$, $B=0.8$, and $C=0.18$ were found experimentally. These results are shown in figure 7.

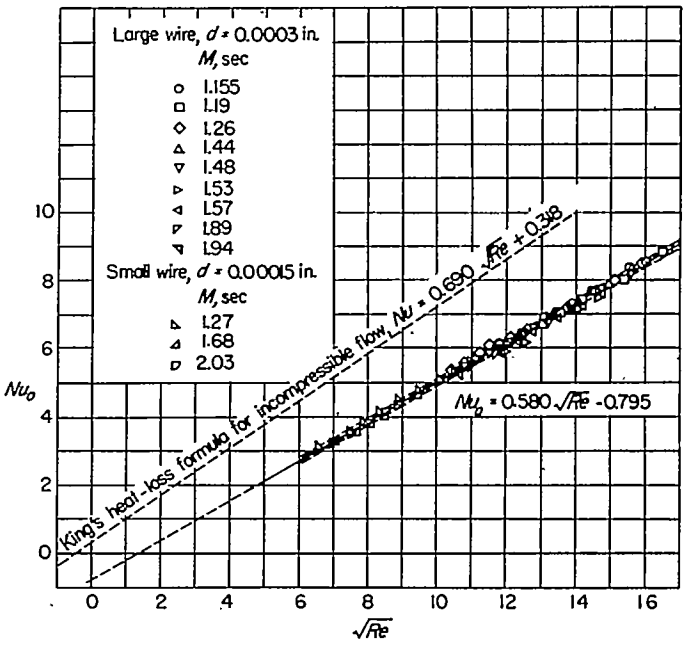

FIGURE 7.—Heat loss of wire at supersonic speeds. $R_e=\frac{\rho u d}{\mu_o}$; $Nu_o=\frac{H}{\pi l \Delta T k_o}$; standard deviation of Nu_o is 0.098.

According to equation (14), the hot-wire responds to mass flow and stagnation temperature, and the fluctuation sensitivities can be computed accordingly. The wire is sensitive to mass-flow fluctuations and to stagnation-temperature fluctuations. If the voltage fluctuations caused by 1-percent mass-flow and 1-percent absolute stagnation-temperature fluctuations are denoted by Δe_m and Δe_T, respectively, the voltage fluctuation across the wire becomes (eqs. (8a) and (8b) of ref. 2)

$$\Delta e=-100\Delta e_m\frac{\Delta(\rho U)}{\overline{\rho U}}+100\Delta e_T\frac{\Delta T_o}{\overline{T}_o} \tag{15}$$

$$\Delta e_m=\frac{IR_w}{100}\phi\frac{a_w'}{2}z \tag{16}$$

$$\Delta e_T=\frac{IR_w}{100}\phi\left(\frac{\eta g}{1+a_e}-0.38ya_w'-\eta Ca_w'\right) \tag{17}$$

where η is defined by equations (13) and ϕ accounts for the nonlinearity of heat loss with temperature and y and z depend on the Reynolds number:

$$\left.\begin{aligned} &\phi=\frac{1}{1-\dfrac{C'a_w'(1+a_w)}{g}} \\ &a_w'=\frac{R_w-R_e}{R_e} \end{aligned}\right\} \tag{18}$$

$$\left.\begin{aligned} &C'=\frac{C}{1-Ca_w'\dfrac{1+a_e}{g}} \\ &g=\alpha T_e \end{aligned}\right\} \tag{19}$$

$$\left.\begin{aligned} 1+a_e&=\frac{R_e}{R_f}\\ 1+a_w&=\frac{R_w}{R_f}\end{aligned}\right\} \tag{20}$$

$$\left.\begin{aligned} y&=\frac{\sqrt{R_e}-2\sqrt{Re_0}}{\sqrt{Re}-\sqrt{Re_0}}\\ \sqrt{Re_0}&\approx 1.3\\ Re&=\frac{U\rho d}{\mu_0}\\ z&=\frac{\sqrt{Re}}{\sqrt{Re}-\sqrt{Re_0}}\end{aligned}\right\} \tag{21}$$

The separation of root-mean-square mass-flow fluctuation and root-mean-square temperature fluctuation and the correlation between the two can be determined by taking measurements of mean-square fluctuations with the wire at different operating temperatures.

The sensitivity coefficients Δe_m and Δe_T and their ratio are given as a function of a_w' in figure 8.

GENERAL DESIGN CONSIDERATIONS

The equipment is intended to indicate turbulent-velocity fluctuations and their time derivatives either at one or at two points in an air stream and to measure mean-square values and mean products of fluctuations and their derivatives. These afford the more commonly known statistical quantities, such as turbulent intensity, turbulent energy, correlation coefficients, scale, and shearing stress. In addition, it is intended that the equipment should provide the basic units to which other circuits and instruments may be attached when it is desired to obtain other statistical quantities. For example, these may be frequency analyzers to obtain the spectrum or statistical analyzers to obtain probability distributions.

Commonly used hot-wire arrangements were also taken into consideration when laying out requirements. These arrangements are the single-wire probe with wire normal to the wind and the ×-wire probe with a pair of wires, one at a positive angle to the wind and one at a negative angle to the wind. These are well-known types used in the measurement of the three mutually perpendicular components of the velocity-fluctuation vector. Since it was known to be necessary in many cases to use two such probes and to compensate them separately for lag, two channels were desirable.

Features that would make possible the measurement of turbulence in high-speed wind tunnels were placed uppermost among design considerations. The extension of response to higher frequencies was therefore the primary requirement. The turbulence level to be measured, on the other hand, is expected to be quite low; therefore the noise level imposes limits on the sensitivity. These requirements suggested the decision in favor of conventional compensation (inverse

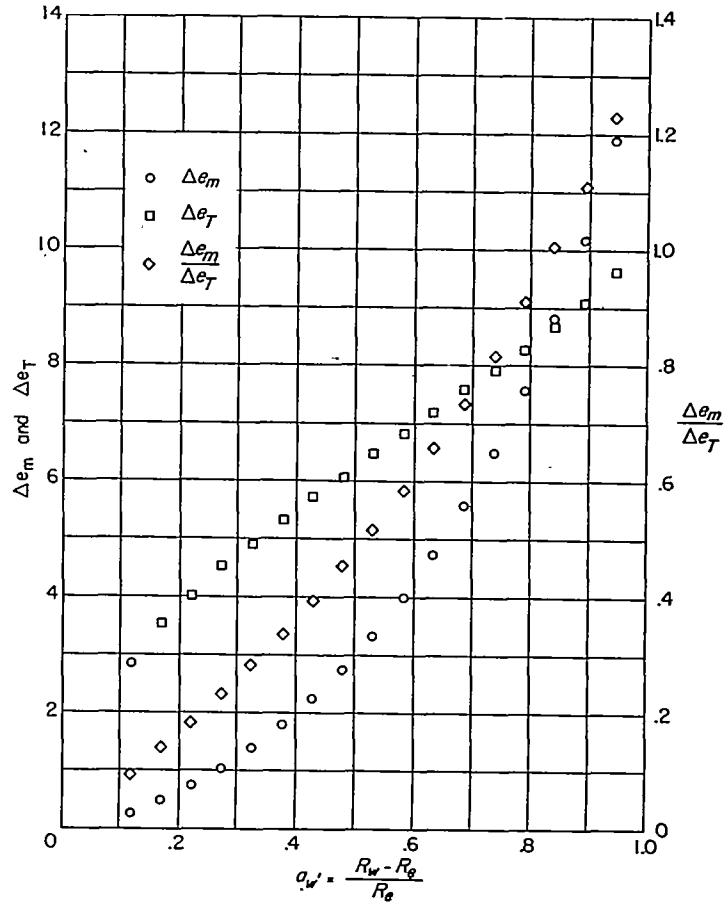

FIGURE 8.—Variation of fluctuation sensitivities with wire temperature in supersonic flow. Tungsten wire with 0.0015-inch diameter was used. Flow conditions: $M=1.73$, $To=293°$ K, and pressure at stagnation temperature was 40 centimeters of mercury.

circuit) instead of a constant-temperature negative feedback system (see section entitled "Compensating Amplifiers").

Early in the work it was decided that the problem of measuring turbulence at very high speeds should be approached by first analyzing and perfecting the fundamental techniques and apparatus necessary for such measurements, rather than by a hurried attempt to place hot-wires in a supersonic stream before the behavior of such wires and their response characteristics were known. Therefore it was decided to build equipment of a permanent type, which would be rugged and easy to service and check. In other words, the object was to avoid operational difficulties that so often plague a temporary laboratory setup. Such qualities become of inestimable value when experiments are undertaken in large supersonic wind tunnels where test time is at a premium. Another advantage is that the equipment then would follow commercial practice; that is, a certain function is performed inside a "box" without special attention from the operator. Because the art of using hot-wires at supersonic speeds is so new, it was felt imperative that the equipment should have as great a versatility as possible. This quality has been achieved in the present equipment to a gratifying degree.

The possibility of using two hot-wire probes at two different points in the flow field, where the operating conditions may

be quite different, led to the use of two independent amplifier channels. If the correlation coefficient is to be measured between two fluctuating quantities, the necessary sum-and-difference signals can then be produced after compensation and amplification. The advantages accruing from the use of grounded rather than ungrounded input circuits and possible means for reversing the polarity led to a decision in favor of push-pull amplifiers in all of the circuits. The direct measurement of the correlation coefficient is made possible by using a ratiometer to read directly the ratio of mean squares of the sum-and-difference signals from two hot-wires. This objective calls for a high-power output square-law detector, a requirement which led to the development of the biased-diode type of squaring circuit. The two independent channels, each built with push-pull amplifiers, naturally permit the measurement of correlation in the ordinary way, namely, by forming the sum and difference of the two signals of the two wires before feeding them to the amplifier. The correlation coefficient of two variable quantities $a(t)$ and $b(t)$ that have zero averages is

$$R_{ab}=\frac{\overline{ab}}{\sqrt{\overline{a^2}}\sqrt{\overline{b^2}}} \tag{22}$$

The bar denotes time average:

$$\bar{x}=\lim_{T\to\infty}\frac{1}{2T}\int_{-T}^{T}x(t)\,dt \tag{23}$$

If the mean square of the sum and difference is formed, the mean product is easy to obtain:

$$\left.\begin{aligned}\Sigma&=\overline{(a+b)^2}\\ \nabla&=\overline{(a-b)^2}\end{aligned}\right\} \tag{24}$$

$$\Sigma-\nabla=4\,\overline{ab} \tag{25}$$

$$\left.\begin{aligned}\sqrt{\overline{a^2}}\sqrt{\overline{b^2}}&=(\Sigma+\nabla)\frac{\xi}{2(1+\xi^2)}\\ \xi&=\frac{\sqrt{\overline{a^2}}}{\sqrt{\overline{b^2}}}\end{aligned}\right\} \tag{26}$$

If the mean-square level of the two signals is adjusted to be identical $\xi=1$ and

$$R_{ab}=\frac{\Sigma-\nabla}{\Sigma+\nabla}=\frac{1-r}{1+r}=f(r) \tag{27}$$

where

$$r=\frac{\nabla}{\Sigma}$$

In this particular case the correlation coefficient becomes a unique function of the ratio of the mean square of the sum and the mean square of the difference.

The direct-current ratiometer is a two-coil instrument with practically no restoring force. The moving system assumes a position so that the opposite torques on the two coils are equal. The torque is proportional to the current in the coil and also to the magnetic field. The pole pieces are shaped in such a way that the magnetic fields vary continuously. The condition for equilibrium depends only on the ratio of the two currents I_1 and I_2. The deflection of the needle β can be expressed approximately by

$$\beta\approx\tan^{-1}\frac{I_1}{I_2}=\tan^{-1}r \tag{28}$$

Since the correlation can be uniquely expressed in terms of the ratio r, the instrument can be scaled directly in correlation coefficient in addition to the ratio scale. With the tangent approximation the correlation scale becomes

$$\left.\begin{aligned}R_{ab}&\approx\tan\left(\beta-\frac{\pi}{4}\right)=\tan\beta'\\ \beta'&=\beta-\frac{\pi}{4}\end{aligned}\right\} \tag{29}$$

giving an almost uniform scale with $R_{ab}=0$ in the center and $R_{ab}=1$ and $R_{ab}=-1$ at the two ends.

Since the equipment was expected to be used under circumstances where there had been little previous experience with respect to wire thermal lag, that is, at supersonic flow, provision has been made to measure the thermal lag of the wire. This is done by the square-wave method described in reference 11. The problem of feeding square-wave current pulses into a relatively low impedance hot-wire circuit necessitated the use of a power amplifier. The presence of a power amplifier, on the other hand, provided a simple solution for control of the hot-wire heating current.

The units of the equipment must perform a large variety of functions that are listed below:

(1) Supplying a controlled heating current to the wires
(2) Measurement of the heating current (0.1-percent accuracy)
(3) Measurement of the hot-wire resistance (mean resistance with 0.05-percent accuracy)
(4) Combination of the voltage output of two wires (sum and difference)
(5) Superposition of square-wave signals on wire-heating current
(6) Amplification of hot-wire signal
(7) Compensation for thermal lag
(8) Rejection of signals of higher frequency than desired
(9) Measurement of root-mean-square signal output of amplifier
(10) Equalization of two compensated output signals
(11) Formation of sum-and-difference signal from two channels
(12) Amplification of combined signals
(13) Differentiation of signal (once or twice) with respect to time
(14) Squaring of a signal
(15) Forming the ratio of two squared signals (mean square)
(16) Supplying known-magnitude root-mean-square signals for calibrating the channels
(17) Supplying known time-constant circuit for calibrating and checking thermal-lag compensation

In addition to these basic functions, the amplifiers must be

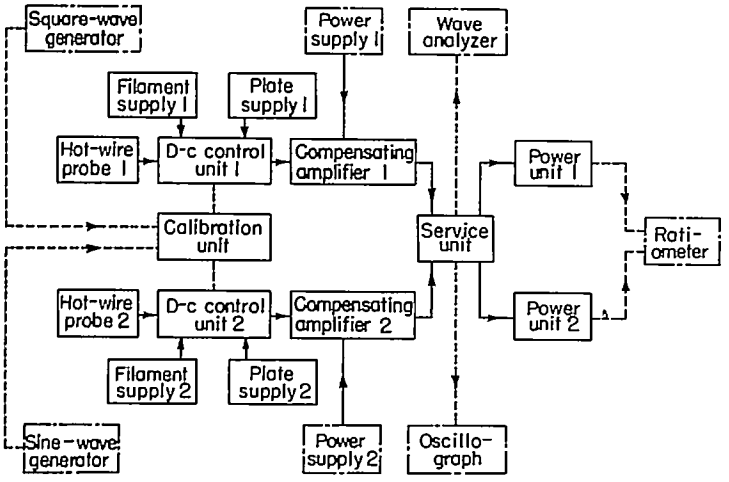

FIGURE 9.—Block diagram of turbulence-measuring equipment.

supplied with appropriate forms of power which are controlled and metered. Sine-wave and square-wave generators are used for calibration purposes. An oscilloscope is used to monitor the output signal. The hot-wire heating current is measured by the voltage drop across a resistor in series with the wire by the aid of a direct-current potentiometer.

The various functions listed above are performed in the different units as follows:

(a) Two control units: (1), (2) partly, (3), (4), and (5)
(b) Two compensating amplifiers: (6), (7), and (8)
(c) One service unit: (9), (10), (11), and metering power for two compensating amplifiers
(d) Two power units: (12), (13), and (14)
(e) One calibration unit: (2) partly, (16), and (17)
(f) Auxiliary equipment including ratiometer: (15)

The block diagram of the equipment is given in figure 9 and the auxiliary equipment is shown by broken lines. A photograph is shown in figure 10. The breakdown of the equipment into units is mainly dictated by the flexibility desired and also by the order of magnitude of signals to be handled. The range of the quantities to be measured was cautiously bracketed and the preliminary design data follow:

Platinum-hot-wire diameter, in	0.00005–0.00025
Tungsten-hot-wire diameter, in	0.00015–0.00030
Hot-wire resistance, ohms	2–100
Hot-wire heating current, ma	10–300
Time constant of thermal lag, milliseconds	[a] 0.1–5.0
Voltage signal from wires, mv	[b] 0.1–100
Output signal from compensating amplifier (maximum output before overloading), v	10–20

[a] In the new equipment the upper limit was only 1.0 millisecond since sufficiently thin wires were used.

[b] Not taking into account thermal-lag effect. (Actual input signal is attenuated additionally by lag involving a factor 2–20.)

The breakdown of the total amplification between (b) and (d) is such that the compensating amplifier has an approximate amplification of 10,000, with an output impedance of 3,000 ohms (each side of push-pull). This results in an output-voltage level of 1 volt for a 100-microvolt input. Further manipulation of the signal, therefore, is performed on a level of the order of 1 volt or more. The power unit has a maximum amplification of the order of 50 and its output is of the order of 30 to 40 volts. The

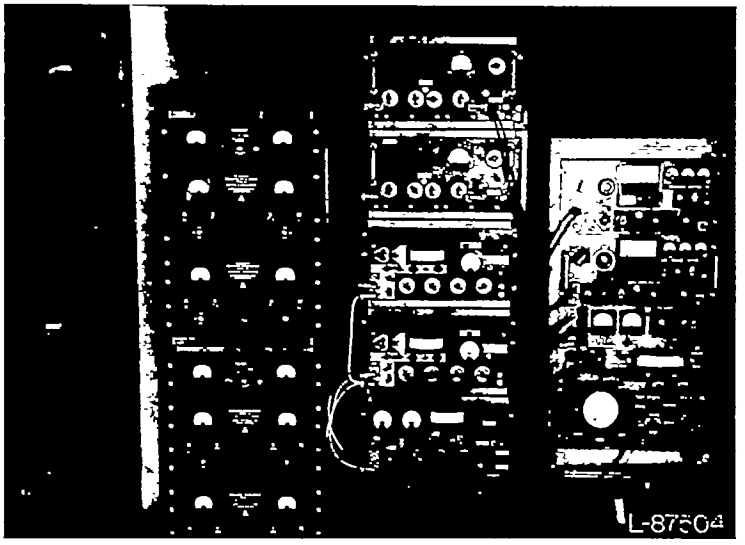

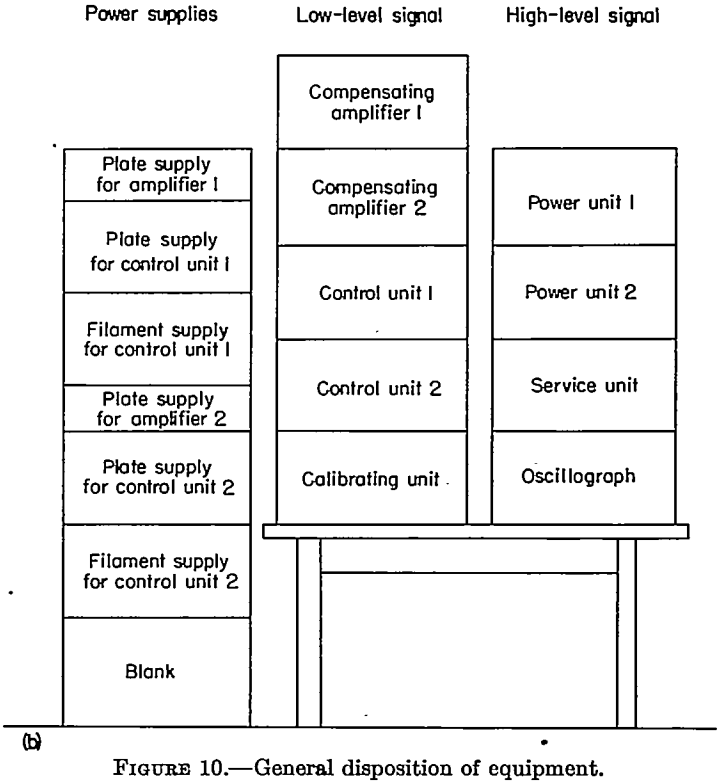

FIGURE 10.—General disposition of equipment.

square detector supplies a current of the order of 0.5 milliampere into a load of 1,500 ohms, which is adequate for the ratiometer. All attenuators have ratio steps of $1:\sqrt{2}$, making a ratio 1:2 after squaring. By manipulation of the attenuator control the readings of the square-type detector are always in the more accurate region of the scale.

In the following section the individual units will be described in detail.

DESCRIPTION OF EQUIPMENT

The parts list for the connectors of the various units is given as table 1. The parts lists for the other components of the circuits are given with the detailed circuit diagrams.

CONTROL UNIT

There are two identical control units, one for each channel. The detailed circuit diagram is given in figure 11. The front

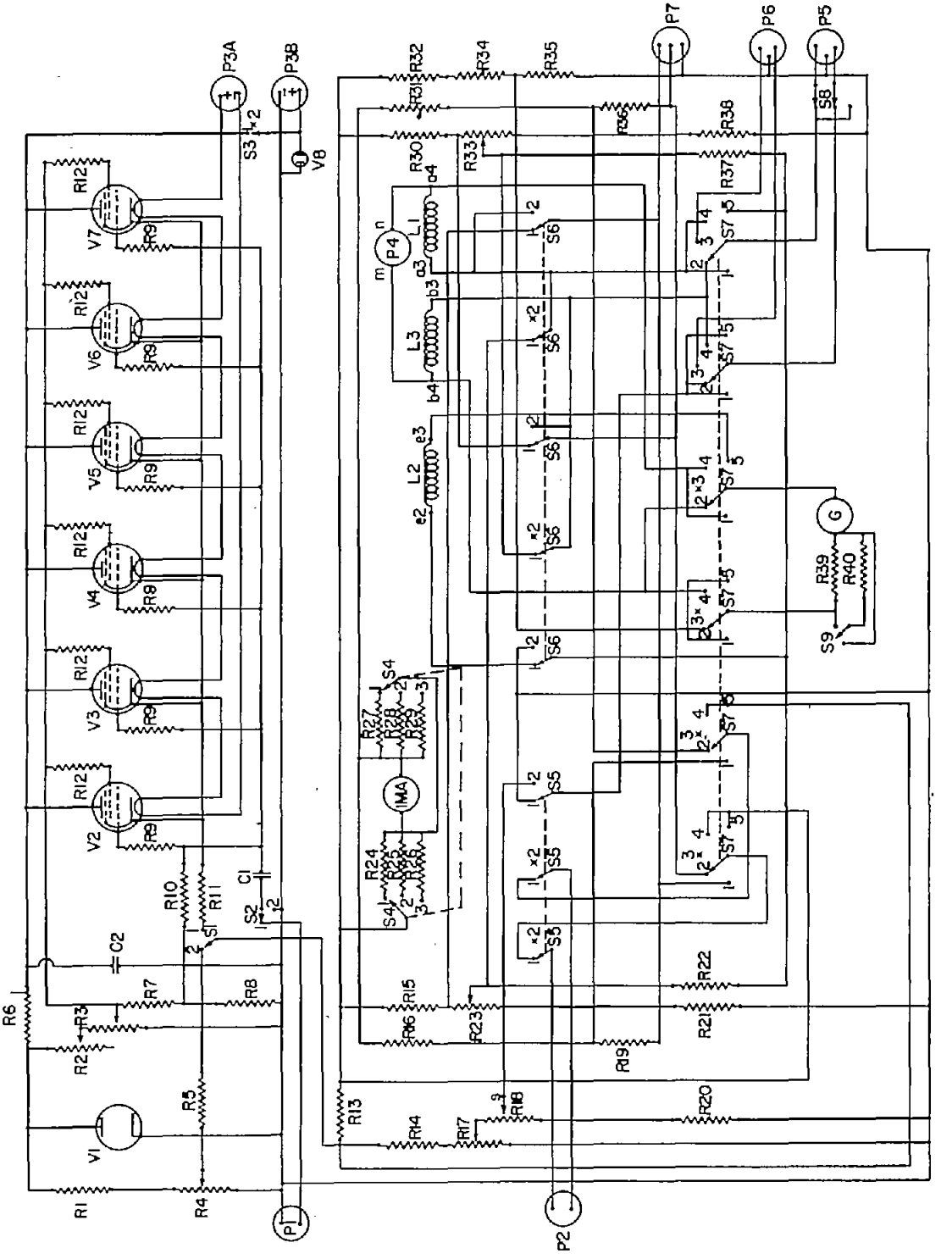
P1
P2
P3A
P3B
P4
P5
P6
P7
V1
V2
V3
V4
V5
V6
V7
V8
L1
L2
L3
G
1MA
S1
S2
S3
S4
S5
S6
S7
S8
S9
C1
C2
R1
R2
R3
R4
R5
R6
R7
R8
R9
R10
R11
R12
R13
R14
R15
R16
R17
R18
R19
R20
R21
R22
R23
R24
R25
R26
R27
R28
R29
R30
R31
R32
R33
R34
R35
R36
R37
R38
R39
R40

Symbol	Description	Value	Rating	Manufacturer	Type	Remarks
V1	Electronic tube			Radio Corp. of Am	OD3	
V2 to V7	Electronic tubes			Radio Corp. of Am	6SL6	
V8	Neon bulb			General Electric Co	NE51	
R1	Resistor, wire-wound	6,000 Ω	10 w			
R2	Potentiometer, linear wire-wound	5,000 Ω	4 w	Mallory Electric Corp	M5MP	
R3	Potentiometer, linear wire-wound	20,000 Ω	4 w	Mallory Electric Corp	M20MP	
R4	Potentiometer, linear wire-wound	2,000 Ω	4 w	Mallory Electric Corp	M2MP	
R5	Resistor, wire-wound	200 Ω	10 w			
R6	Resistor, wire-wound	6,000Ω	10 w			
R7	Resistor, wire-wound	35,000 Ω	10 w			
R8	Resistor, wire-wound	25,000 Ω	10 w			
R9	Resistor, carbon	2,000 Ω ±5%	½ w			
R10	Resistor, carbon	82,000 Ω±5%	1 w			
R11	Resistor, wire-wound	100 Ω±5%	10 w			
R12	Resistor, carbon	5,000 Ω	½ w			
R13	Resistor, wire-wound noninductive	4.717 Ω±0.1%	300 ma	Shallcross Manufacturing Co		Special.
R14	Resistor, carbon	3,000 Ω±1%	2 w			
R15, R30	Resistor, wire-wound	55,000 Ω±0.1%	1 w	Shallcross Manufacturing Co	BX103E	
R16, R31	Resistor, wire-wound	500 Ω±0.5%	150 ma	Shallcross Manufacturing Co	BX116-L	Each comprised of five series resistors.
R17	Potentiometer, linear wire-wound	2,000 Ω	4 w	Mallory Electric Corp	M2MP	
R18	Potentiometer, linear wire-wound	200 Ω	4 w	Mallory Electric Corp	M200P	
R19, R35	Resistor, wire-wound noninductive	10 Ω±0.1%	310 ma	General Radio Co	500B	
R20	Resistor, Carbofilm	2,000 Ω±1%	1 w			
R21, R38	Resistor, Carbofilm	650 Ω±1%	1 w			
R22, R37	Resistor, wire-wound noninductive	1,000 Ω±0.1%	30 ma	General Radio Co	500H	
R23, R33	Potentiometer, carbon	100 Ω	2 w			
R24, R27	Resistor, wire-wound	0.2 Ω±1%				Built in laboratory.
R25	Resistor, wire-wound	2.92 Ω±1%				Built in laboratory.
R26, R28	Resistor, wire-wound	1.97 Ω±1%				Built in laboratory.
R29	Resistor, wire-wound	1.44 Ω±1%				Built in laboratory.
R30	See R15.					
R31	See R16.					
R32	Resistor, wire-wound noninductive	5,000 Ω±0.1%	14 ma	General Radio Co	500M	
R33	See R23.					
R34	Resistor, carbofilm	100 Ω±1%				
R35	Resistor, four-decade	(a) 1,000 Ω±0.1% in 10 steps		General Radio Co	510D	
		(b) 100 Ω±0.1%		General Radio Co	510C	
		(c) 10 Ω±0.25%		General Radio Co	510B	
		(d) 1 Ω±1%		General Radio Co	510A	
R36	See R19.					
R37	See R22.					
R38	See R21.					
R39	Resistor, carbon	100,000 Ω±5%	½ w			
R40	Resistor, carbon	5,000 Ω±5%	½ w			
C1	Capacitor	4 μf	100 v d.c.	Sprague Electric Co	Vitamin Q	
C2	Capacitor	0.5 μf	450 v d.c.	Aerovox Corp		
L1, L2	Inductive coil, toroid	0.35 mh	By 35 ma	Burnell & Co	TC 1-350	
L3	Inductive coil	0.5 mh	By 18 ma	Burnell & Co	TC 1-1500	
S1, S2, S3	Toggle switch, one-pole double-throw					Positions: 50 ma, 100 ma, and 500 ma.
S4	Lever-type switch	3 positions		Centralab Div., Globe-Union, Inc	1454	
S5, S6	Rotary switch	6 poles, 3 positions		Mallory Electric Corp	3253 J	Positions: S5: 1, turbulence 2, square S6: 1, match 2, off
S7	Rotary switch	8 poles, 5 positions		Centralab Div., Globe-Union, Inc	Jv 9007	Positions: 1, A; 3, B; 3, ext; 4, diff; 5, sum.
S8	Toggle switch.					Built in laboratory.
S9	Telephone-type key switch					
G	Galvanometer	15-0-15 μa		Sensitive Research Instrument Corp	Jw	
IMA	Milliammeter	0 to 1 ma		Weston Electrical Instrument Corp	301	

FIGURE 11.—Control unit.

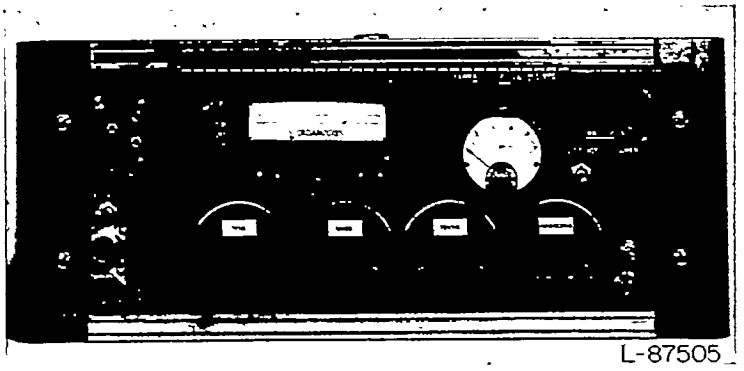

FIGURE 12.—Control unit, front view.

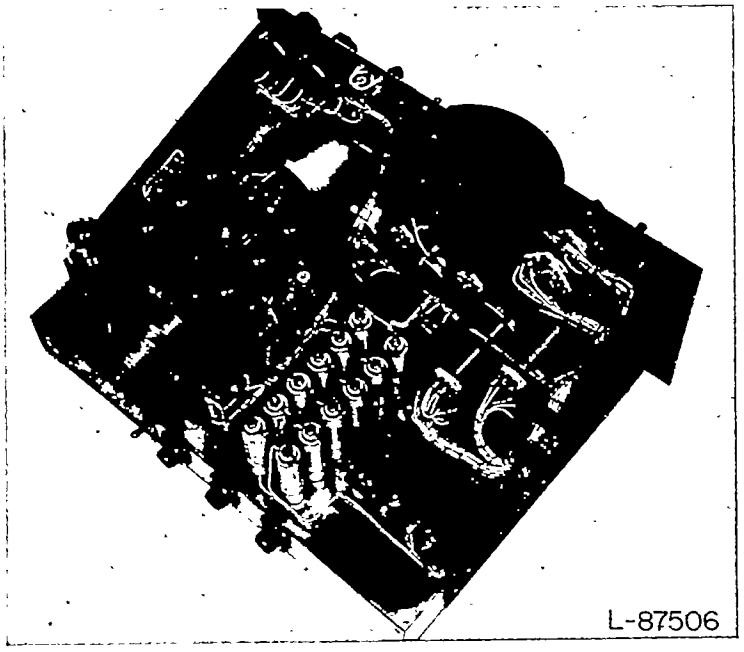

FIGURE 13.—Control unit, top view.

view of the control unit is shown in figure 12 and the top view of the wiring is given in figure 13. The main functions of the control unit are:

(1) Control of heating current in the wires
(2) Measurement of wire resistance (mean) under both hot and cold conditions
(3) Combination of wire signals before feeding them to the compensating amplifier
(4) Superposition of square-wave current pulses to the heating current for measurement of thermal lag

One end of each hot-wire is always connected to the ground, and one side of the square-wave generator is also grounded. This is considered a rather important design feature of the equipment, especially when high frequencies are occurring in the signal, because neither floating wires nor floating power supplies could be tolerated.

The circuit consists of three parts:

(a) Current control
(b) Multiple bridge
(c) Switching arrangement

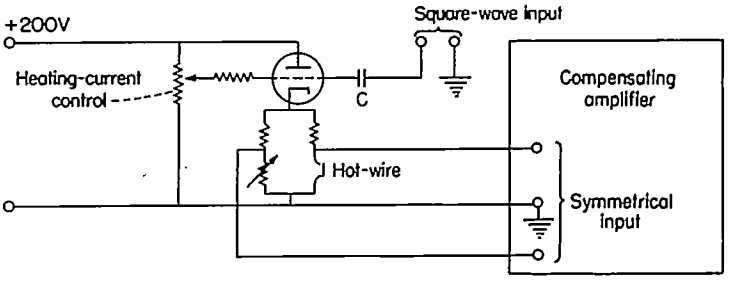

FIGURE 14.—Heating-current control and square-wave feeding system.

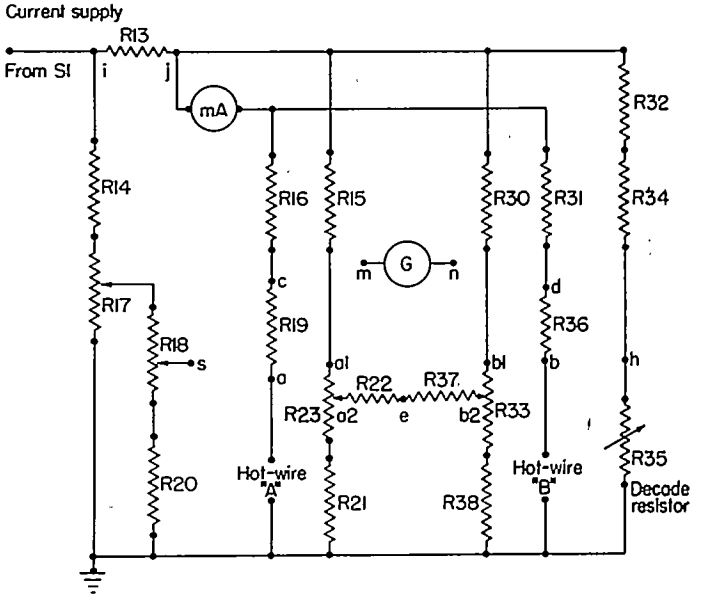

FIGURE 15.—Multiple bridge in control unit.

The heating current is controlled by six power tubes (50L6-G) and the multiple bridge represents the cathode load (see fig. 14). This cathode-follower type of operation greatly facilitates the superposition of any current fluctuations such as square waves on the control grids. The current is controlled by the grid bias from a stabilized voltage divider.

The measurement of cold resistance of the wire requires very small currents (1 to 10 milliamperes). Special provisions were made to feed a small current to the wires directly from the voltage divider, since the tubes pass a larger current even at zero grid bias voltage.

In the original version the power tubes were connected as triodes; in the new form, however, they are used as pentodes and current control is effected by both control grid and a screen grid, thus providing a large range of current. This change was made concurrently with replacing the storage batteries by electronically controlled power supplies.

The multiple bridge consists of six parallel arms (fig. 15). Each arm acts as a voltage divider and a certain positive potential with respect to ground appears on points, s, a, a_2, b_2, b, and h. The resistance-measuring arm consists of R32, R34, and R35. The bridge ratio is 10:1 and resistance values up to 100 ohms can be measured in 0.01-ohm steps.

By appropriate switching the direct-current potential

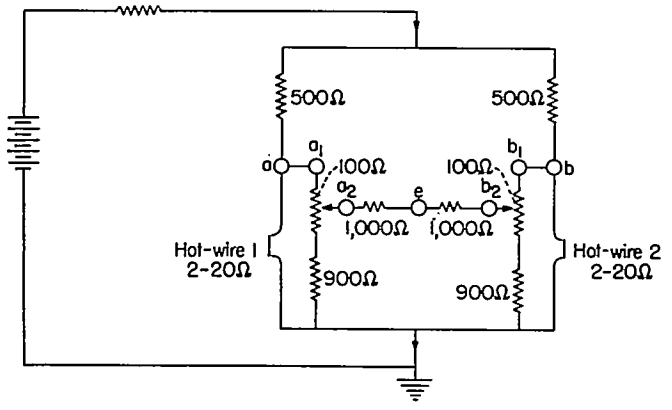

FIGURE 16.—Matching circuit.

differences can be detected by the galvanometer, thus giving resistance measurement or resistance comparison (e. g., two wire probes). The alternating-current potential fluctuations can be fed to the compensating amplifier both separately and in appropriate combinations. The heating current is accurately measured as a voltage drop across standard resistors by means of a direct-current potentiometer (located in the calibration unit). The standard resistors R19 and R36 are placed in series with each wire and an extra one R34 is in series with the whole bridge. The value of the latter is chosen to give the same voltage drop as the individual ones if two hot-wires are used. The principal switch S7 has five combinations for measuring either one of two single wires, the sum and difference of them, or an external calibrating signal.

The combination of two signals before amplifying requires the use of rather well matched wires. If the two wires have slightly unequal lengths, and therefore resistances (less than 10 percent), a special matching circuit (fig. 16) can reduce the effective length of the wire by tapping off a reduced potential from points a_2 and b_2. Since the compensating amplifier has a push-pull input, neither side requires grounding. This gives the possibility of measuring the difference output of two wires. The half sum of the signal from the two wires can be obtained by tapping off the midpoint of a 1:1 voltage divider between the two hot-wire potentials (point e). In this way the sum-and-difference signals can be obtained before amplification, and the correlation coefficient can be measured in the conventional way.

On the other hand, if the correlation coefficient is measured by the ratiometer, each probe is connected to one separate control unit, each signal is amplified and compensated separately, the sum and difference are formed in the service unit, and the mean squares are formed by the power units. This latter method is desirable if the two hot-wire probes must operate at two different points in the flow where the mean velocities, and therefore time constants, are widely different.

The square-wave calibration of thermal lag requires a separate bridge arm. The temperature (resistance) fluctuations can be obtained from a balanced bridge even in the presence of an alternating-current component in the bridge current. Unfortunately, the decade resistors used in the calibrated bridge arm R35 do not have good high-frequency response; therefore the potential for the square-wave tests is taken from the uncalibrated bridge arm (from point s). Potentiometers R17 and R18 are carbon potentiometers. If the voltage from the wire alone is used, this signal contains an undesired square-wave contribution that gives "spikes" when compensated (differentiation), so the bridge arrangement is absolutely necessary. Special chokes L1, L2, and L3 protect the galvanometer from the square-wave component of the heating current, and the heating-current measurement by the direct-current potentiometer is also suspended during the square-wave test.

COMPENSATING AMPLIFIERS

The compensating amplifier is the most critical part of the hot-wire equipment. An unconventional layout is necessary because of two extreme requirements. First, the level of the input signal is extremely low; therefore the question of thermal noise becomes of very great importance. Second, the electronic compensation of the thermal lag of the hot-wire requires a special frequency-response characteristic that can be adjusted with high accuracy according to time-constant values. These features naturally can be obtained only by additional gain and extended-frequency band width.

The operating-frequency range is 2 to 80,000 cycles per second; therefore large interstage coupling condensers are needed for good low-frequency response which then necessitates special disposition and mounting features to avoid parasitic capacitances to ground and loss of gain at higher frequencies.

The hot-wire is a low-impedance source (2 to 20 ohms); therefore the thermal noise originates primarily from the first amplifier stage. The use of transformer coupling in order to improve signal-to-noise ratio could not be extended to both lower and upper ends of the frequency band. Another method for improving impedance matching between source and amplifier is the use of high-impedance metal-coated quartz fibers as hot-wires. No successful results have yet been published.

The thermal noise is lower for triodes than for pentodes and the equivalent noise-generating resistance decreases inversely proportional to the transconductance of the tube. This led to the choice of 6J4 tubes in the first stage of the original equipment. In the new equipment, however, they were changed to Western Electric 417A, which showed both greater stability and lower equivalent thermal noise. Since the high transconductance always involves close cathode-grid spacing, these tubes are rather microphonic. This fact promoted the need for the special antimicrophonic suspension used for the first stage.

The thermal lag of the wire produces an attenuation and a phase shift. The frequency response of the wire with complex notation follows:

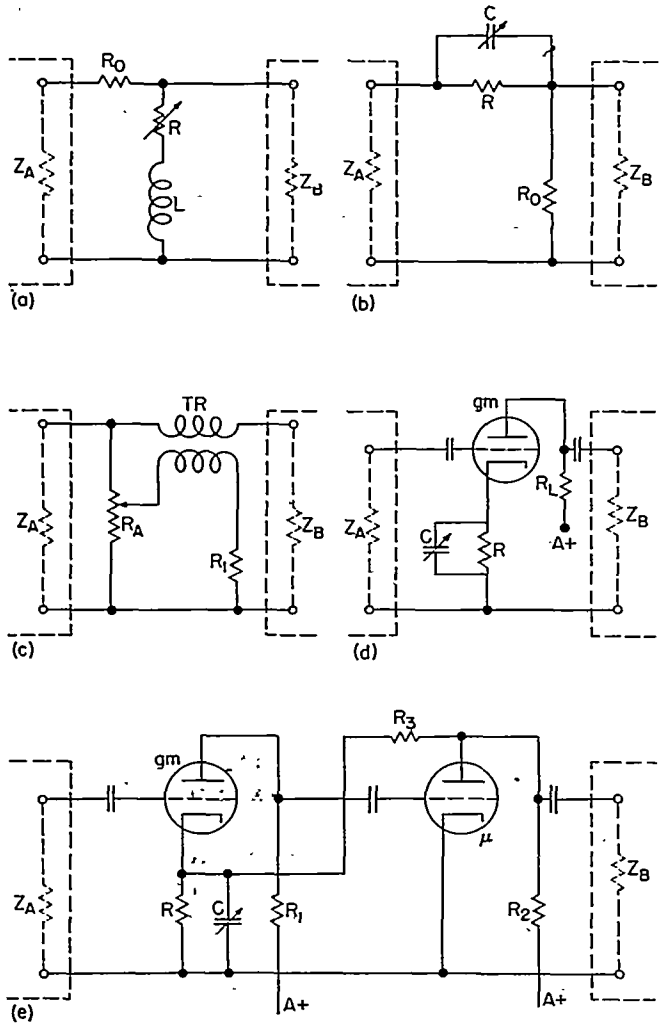

(a) Inductance resistance.
(b) Capacitance resistance.
(c) Transformer.
(d) Negative-feedback resistance capacitance.
(e) Improved form of system (d).

FIGURE 17.—Compensation systems.

$$\left.\begin{aligned}\frac{e}{e_s}&=\frac{1}{1+2\pi ifM}\\ i&=\sqrt{-1}\end{aligned}\right\} \tag{30}$$

Here e_s is proportional to the velocity (or temperature) fluctuation and e is the actual distorted voltage output of the wire. The compensation therefore must have a complex frequency response $1+2\pi ifM$. This means that the compensating circuit also has a characteristic time constant and the amplification becomes simply proportional to the frequency if the frequency is large ($2\pi fM \gg 1$). Such circuits with a time constant can be obtained in many ways; therefore the compensation systems are numerous. The several types that have been adopted are shown in figure 17. These are described briefly as follows:

(a) Inductance-resistance compensation (fig. 17(a)). This is the earliest type of compensation (ref. 8) where $L/R=M$ with the additional requirement $R_0 \gg R$. The large value of L necessitates the use of a large inductance choke. Frequency limitation is mainly due to the resonant frequency of the choke. The time constant is controlled by R which in turn also alters the amplification.

(b) Capacitance-resistance compensation (fig. 17(b)). This is the most commonly used type. Compensation is controlled by the variable condenser C. Requirements are $M=RC$ and $R_0 \ll R$. The main disadvantage is that C is floating above ground potential. The advantage compared with type (a) is that the amplification does not change with compensation setting.

(c) Transformer compensation (ref. 11 and fig. 17(c)). The transformer adds a differentiated signal sufficient to restore the loss of signal from the wire. The advantage is no loss of gain. The disadvantage is the magnetic pickup and resonance of the transformer.

(d) Negative feedback resistance-capacitance compensation (ref. 12 and fig. 17(d)). The equivalent circuit is identical with type (b) but has the advantage of being a low-impedance circuit. The condenser is grounded on one side (or close to ground in a push-pull circuit). The time constant $M=RC$, and the gain is R_L/R. The total range of compensation is $1+g_mR$, where g_m is the transconductance of the tube. The ceiling-to-floor ratio can be made 20 to 30 without making the minimum gain of the stage less than unity.

(e) An improved form of type (d) developed for the present equipment (fig. 17(e)). The feedback ratio is increased by

$$1+\frac{\mu R_1}{R+R_3}$$

where μ is the amplification of the second stage. The total feedback ratio can be boosted to a value between 200 and 300, compared with 20 to 30 for type (d), and the minimum gain across the two stages is still approximately 10.

There is also an entirely different approach to the compensation problem, namely, the constant-temperature feedback system shown schematically in figure 18. The hot-wire is placed in a bridge and the unbalance voltage is amplified and fed back to the bridge to suppress the temperature changes of the wire. The system is discussed in detail in references 13 and 14.

For the present equipment, type (e) compensation was developed incorporating the advantages of types (b) and (d) but not having all of their shortcomings. The ideal compensation would require ever-increasing response proportional to frequency (at high frequencies). Since there is no amplifier which has an unlimited increase in gain with frequency rise, the compensation has an ultimate limit. The working range of compensation can easily be represented by the ratio between basic amplification ("floor") and the maxi-

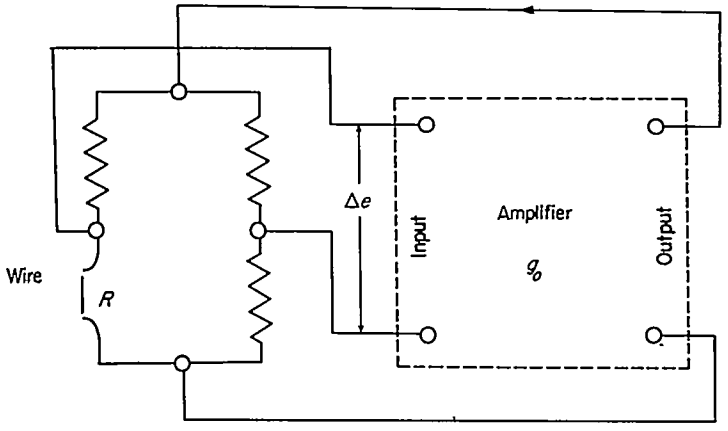

FIGURE 18.—Constant-temperature feedback system.

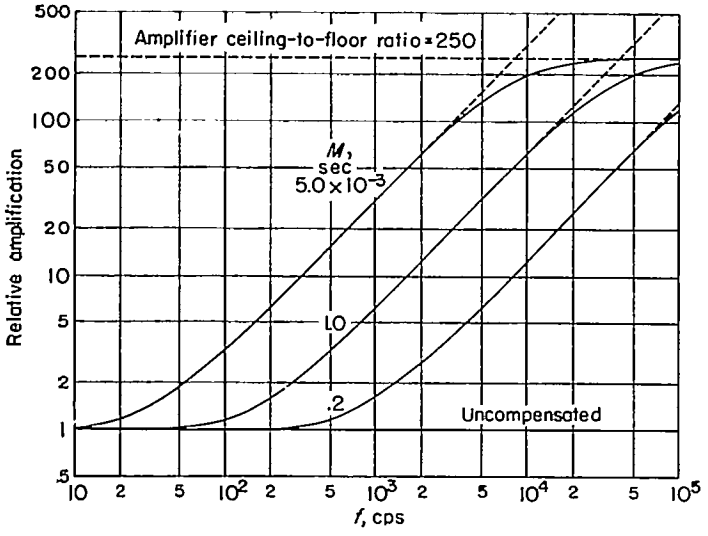

FIGURE 19.—Range of compensation.

mum amplification of the compensating circuit ("ceiling"). The transition curve between the two levels gives the compensation characteristic (see fig. 19). By a suitable choice of circuitry a great part of this "volume" can be used for useful compensation. The ratio between floor (0-frequency) (in fig. 19 shown as "uncompensated") and ceiling (∞-frequency) amplification depends on the circuit constants. In circuit (b) it is simply R/R_0 and in circuits (d) and (e) it is identical to the feedback ratio K. In the case of circuit (d) the floor-ceiling ratio is not more than 20:30. This type of circuit is therefore suitable only for small amounts of compensation. In the present circuit (type (e)) the factor chosen was 250. This gives a satisfactory compensation up to a ratio of 100 ($2\pi fM=100$). Figure 19 shows how the ideal (dashed line) and real (full line) compensation characteristics compare.

Using the usual resistance-capacitance input coupling, the noise is mainly generated in the first stage of the amplifier and consists mostly of tube thermal noise. The equivalent

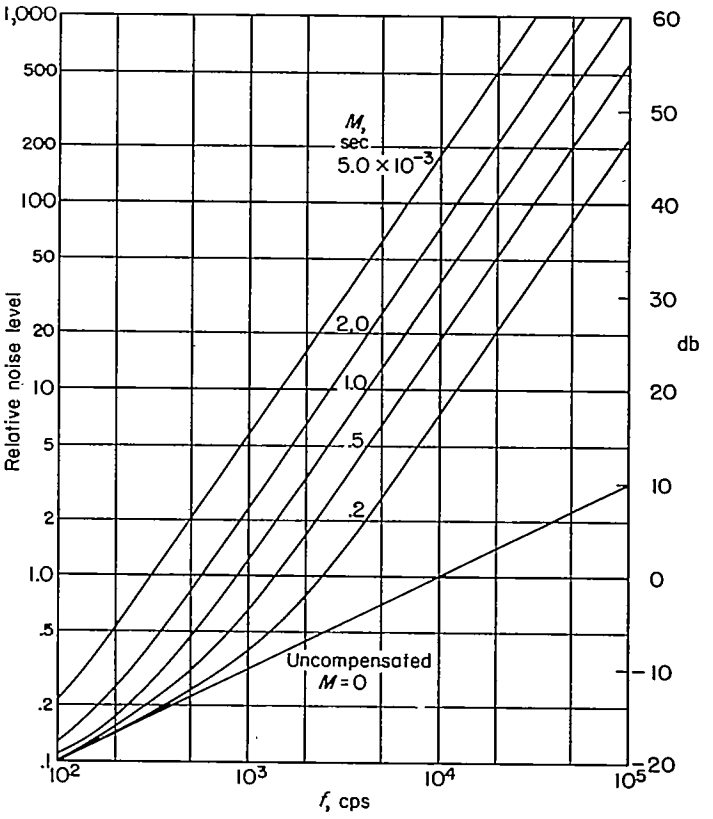

FIGURE 20.—Theoretical noise level of compensating amplifiers as compared with 10-kilocycle band-width amplifier.

noise-generating resistance was studied on single tubes. It was found that 6J4 tubes had 1,200 to 1,700 ohms and 417A tubes, 400 to 700 ohms. Naturally, the push-pull input doubles that value for the amplifier. On selected tubes the noise is white Gaussian noise. If the frequency response of the amplifier were flat, the noise power would increase only proportional to the band width. The time-constant compensation means additional amplification at high frequencies and the white noise is amplified too. The result is a great increase of noise, and the noise voltage increases proportional to the 3/2 power of the band width and proportional to the time constant M. Figure 20 shows the theoretical noise level (voltage) of a compensated hot-wire amplifier compared with a flat-frequency-response amplifier with a band width of 10,000 cycles per second. The noise root-mean-square amplitude of the latter is taken as unity. Every turbulent-energy spectrum measured has a maximum at a relatively low frequency, and the turbulence has an energy spectrum strongly decreasing with increasing frequency. This means that the signal submerges into the noise at some frequency value.

The simplified circuit diagram of the amplifier is given in figure 21. The amplifier consists of five stages. All stages are in a push-pull arrangement to enable the handling of signals from ungrounded sources. The symmetry of the

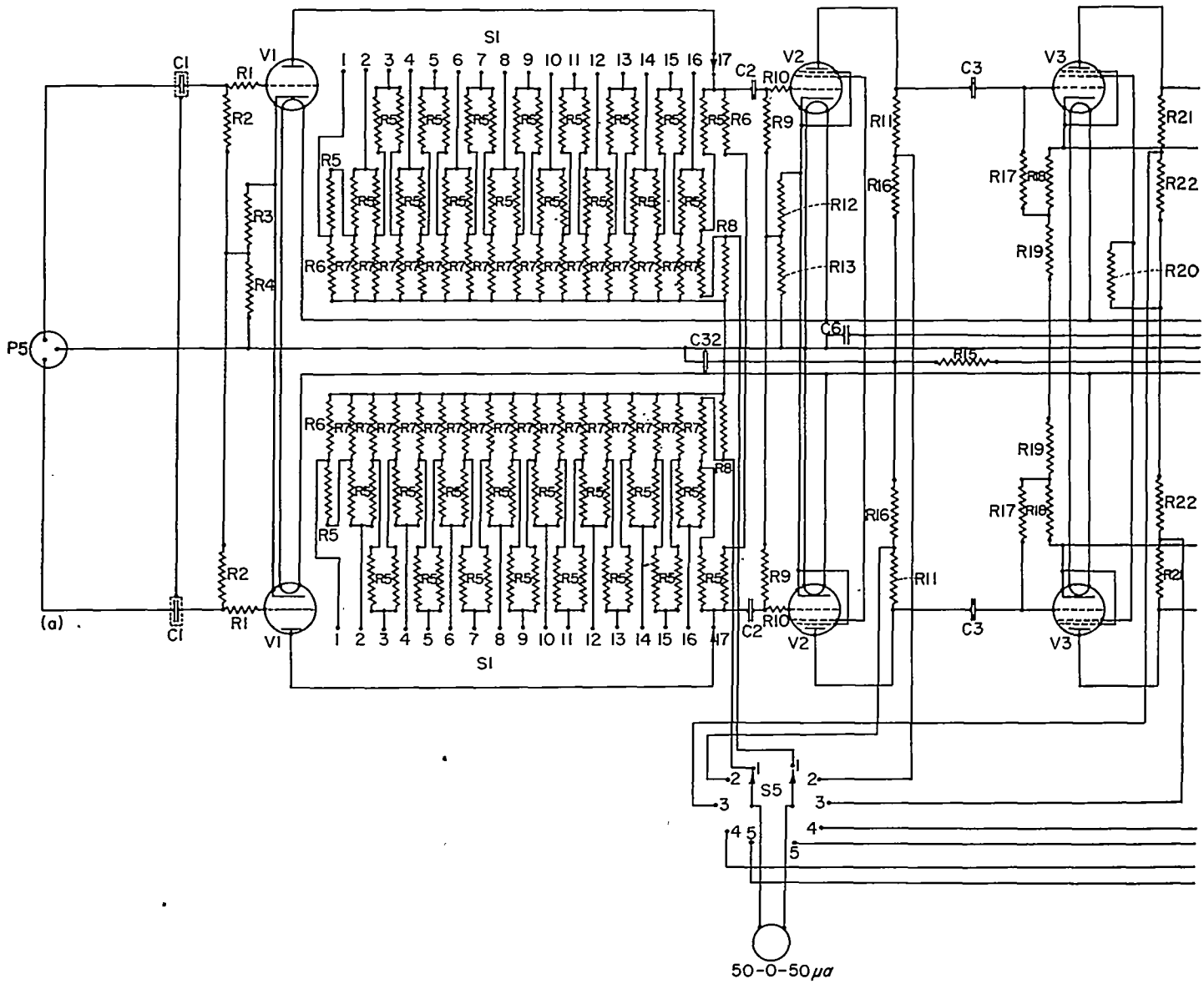

Symbol	Description	Value	Rating	Manufacturer	Type
V1	Electronic tube *			Western Elec. Co., Inc.	417A
V2, V3, V4	Electronic tube *			Radio Corp. of Am.	6AK5
V5	Electronic tube *			Radio Corp. of Am.	6AK6
V6	Neon tube			General Elec. Co.	NE51
C1	Capacitor	4.0 μf	100 v d. c.	Tobe Deutschmann Corp.	DM104
C2, C3, C4	Capacitor	0.5 μf	600 v d. c.	Cornell-Dubilier Elec. Corp.	Bath tube
C5	Capacitor	1.0 μf	600 v d. c.	Cornell-Dubilier Elec. Corp.	Bath tube
C6	Capacitor	0.5 μf	600 v d. c.	Aerovox Corp.	Tubular
C7	Capacitor	0.0005 μf±1%	600 v d. c.	Electro-Motive Mfg. Co., Inc.	Elmenco mica
C8	Capacitor	0.005 μf±1%	600 v d. c.	Electro-Motive Mfg. Co., Inc.	Elmenco mica
C9	Capacitor	0.1 μf±1%		Aerovox Corp.	
C10, C28	Capacitor	0.007 μf±5%	600 v d. c.	Electro-Motive Mfg. Co., Inc.	Elmenco mica
C11, C29	Capacitor	0.0022 μf±5%	600 v d. c.	Electro-Motive Mfg. Co., Inc.	Elmenco mica
C12, C26	Capacitor	0.004 μf±5%	600 v d. c.	Electro-Motive Mfg. Co., Inc.	Elmenco mica
C13, C27	Capacitor	0.0012 μf±5%	600 v d. c.	Electro-Motive Mfg. Co., Inc.	Elmenco mica
C14, C24	Capacitor	0.0022 μf±5%	600 v d. c.	Electro-Motive Mfg. Co., Inc.	Elmenco mica

Symbol	Description	Value	Rating	Manufacturer	Type
C15, C25	Capacitor	0.0007 μf±5%	600 v d. c.	Electro-Motive Mfg. Co., Inc.	Elmenco mica
C16, C22	Capacitor	0.001 μf±5%	600 v d. c.	Electro-Motive Mfg. Co., Inc.	Elmenco mica
C17, C23	Capacitor	0.00033 μf±5%	600 v d. c.	Electro-Motive Mfg. Co., Inc.	Elmenco mica
C18, C20	Capacitor	0.0007 μf±5%	600 v d. c.	Electro-Motive Mfg Co., Inc.	Elmenco mica
C19, C21	Capacitor	0.00022 μf±5%	600 v d. c.	Electro-Motive Mfg. Co., Inc.	Elmenco mica
C30	Capacitor, electrolyte	3,000 μf	15 v d. c.	Cornell-Dubilier Elec. Corp.	UP3M-15
C31	Capacitor, electrolyte	80 μf	450 v d. c.	Cornell-Dubilier Elec. Corp.	UP80450
C32, C33	Capacitor, electrolyte	40 μf	450 v d. c.	Cornell-Dubilier Elec. Corp.	
R1	Resistor, carbon	100 Ω±1%	½ w		
R2	Resistor, wirewound	100,000 Ω±1%	1 w	Western Elec. Co., Inc.	
R3	Resistor, wirewound	24 Ω±1%	1 w	Western Elec. Co., Inc.	
R4	Resistor, wirewound	1,500 Ω±5%	5 w	Ohmite Mfg Co.	Brown Devils
R5	Resistor, wirewound	1,500 Ω±1%	1 w	Western Elec. Co., Inc.	
R6	Resistor, wirewound	8,750 Ω±1%	1 w	Western Elec. Co., Inc.	
R7	Resistor, wirewound	25,000 Ω±1%	1 w	Western Elec. Co., Inc.	
R8	Restor, wirewound	300 Ω±1%	1 w	Western Elec. Co., Inc.	

* Matched to each other.

FIGURE 21.—Compensating amplifier.

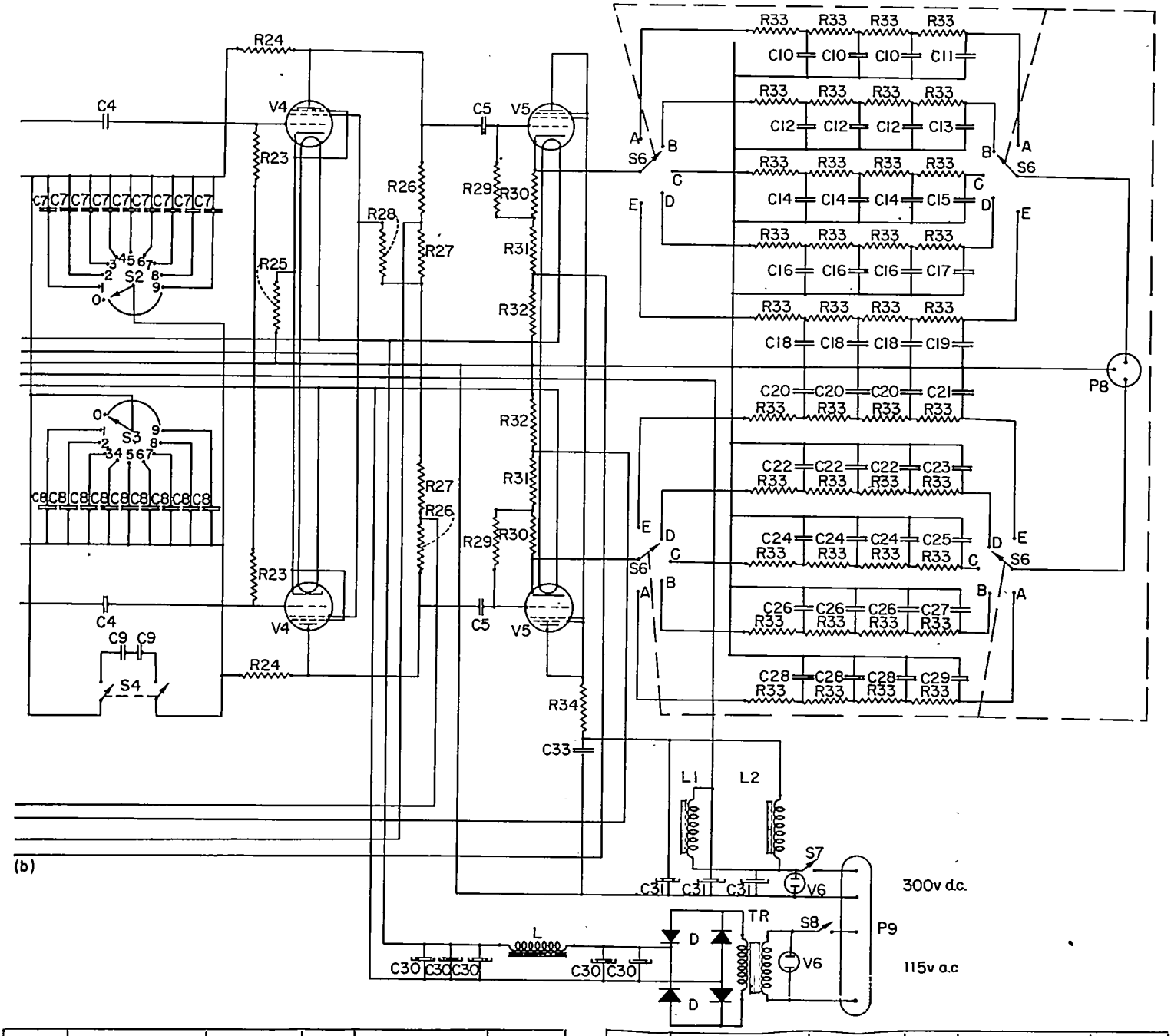

Symbol	Description	Value	Rating	Manufacturer	Type
R9	Resistor, Carbofilm	1,000,000 Ω±1%	½ w		
R10	Resistor, Carbofilm	1,000 Ω±1%	½ w		
R11	Resistor, Carbofilm	15,000 Ω±1%	1 w		
R12	Resistor, Carbofilm	100 Ω±1%	1 w		
R13	Resistor, Carbofilm	1,000 Ω±1%	1 w		
R14	Resistor, carbon	120 Ω	½ w		
R15	Resistor, Carbofilm	1,800 Ω±5%	10 w	Ohmite Mfg. Co.	Brown Devils
R16	Resistor, Carbofilm	22 Ω±5%	½ w		
R17	Resistor, Carbofilm	220,000 Ω±1%	½ w		
R18	Resistor, Carbofilm	200 Ω±1%	1 w		
R19	Resistor, Carbofilm	5,000 Ω±1%	1 w		
R20	Resistor, Carbofilm	5[illegible],000 Ω±5%	1 w		
R21	Resistor, Carbofilm	39,000 Ω±1%	2 w		
R22	Resistor, Carbofilm	22 Ω±5%	½ w		
R23	Resistor, Carbofilm	220,000 Ω±1%	½ w		
R24	Resistor, Carbofilm	100,000 Ω±1%	1 w		
R25	Resistor, Carbofilm	1,000 Ω±1%	1 w		
R26	Resistor, Carbofilm	20,000 Ω±1%	1 w		
R27	Resistor, Carbofilm	22 Ω±5%	½ w		
R28	Resistor, Carbofilm	20,000 Ω±5%	1 w		
R29	Resistor, Carbofilm	220,000 Ω±1%	½ w		
R30	Resistor, Carbofilm	5,000 Ω±1%	1 w		
R31	Resistor, Carbofilm	10,000 Ω±1%	1 w		
R32	Resistor, Carbofilm	10 Ω±5%	½ w		
R33	Resistor, Carbofilm	680 Ω±5%	½ w		
R34	Resistor, Carbofilm	1,000 Ω±10%	5 w	Ohmite Mfg. Co.	Brown Devils

Symbol	Description	Value	Rating	Manufacturer	Type
L	Secondary winding of filament transformer	25.6 v	1 amp	Merit Coil & Transformer Corp.	
L1, L2	Choke	18 h	80 ma	The Halldorson Co.	
TR	Filament transformer	12.6 v	2 amp	Merit Coil & Transformer Corp.	
D	Rectifier, selenium-bridge type	3.8 amp	18 v	The DoAll Co.	Selectron U1B1C1
S1	Switch	2 poles, 17 positions		Centralab Div., Globe-Union, Inc.	JV9004
S2, S3	Switch	1 pole, 10 gradually shortening positions		Centralab Div., Globe-Union, Inc.	P18D
S4	Toggle switch, double-pole double-throw				
S5	Switch	Nonshortening 2 poles, 6 positions		Mallory Electric Corp.	3226J
S6	Switch	4 poles, 5 positions		Centralab Div., Globe-Union, Inc.	2514
S7, S8	Toggle switch, one-pole one-throw.				
50-0-50	Microammeter	50-0-50 μa		Weston Electrical Instr. Corp.	301

FIGURE 21.—Concluded.

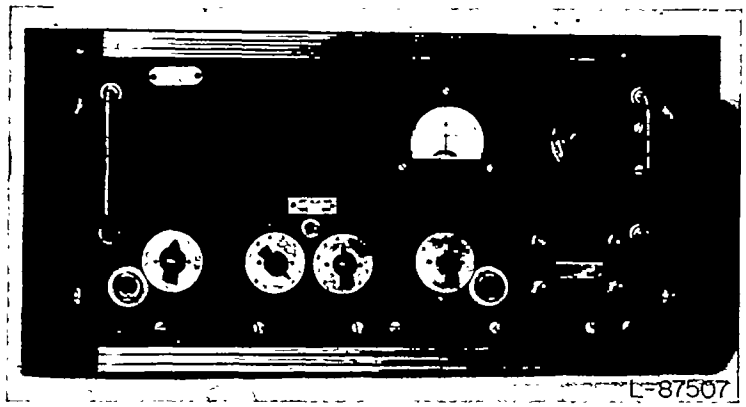

FIGURE 22.—Compensating amplifier, front view.

push-pull arrangement has additional benefits in stability and freedom from hum. The total amplification without compensation is approximately 15,000. The compensation adds another factor of 250 making the total amplification of high frequencies a maximum of 2.5×10^6. The breakdown of stages follows. First stage: Low-noise triode, approximate gain 20. Second stage: High-gain pentode stage, amplification approximately 50. Third and fourth stages: Amplification without compensation approximately 20, with compensation approximately 5,000. Fifth stage: Cathode follower, approximate gain 0.5.

The maximum signal occurs in the fourth stage and overload occurs when the output signal is of the order of 20 volts root mean square. The gain control is between the first and second stages. It is a constant-impedance, double T, ladder-type attenuator with 17 steps having the voltage ratio $1:\sqrt{2}$. This is convenient since it gives a double amplitude in the output of a square detector on the next higher step. The original equipment had LC-type low-pass filters. However, in the new form RC filters were adopted since they are easier to match for the two identical channels and have no overshoot. The output is sufficient to drive a high-impedance thermocouple circuit for all except the lowest level turbulence measurements. The proper balance of the individual stages is monitored by a small meter on the front panel. The tubes are all heated with direct current and the plate supply is a conventional regulated power supply (300 volts, 100 milliamperes) with additional filtering incorporated in the compensating-amplifier unit. Stability of the amplifier was substantially improved by using small series resistors in all grid circuits. Slow oscillations (motorboating) were eliminated by a low-frequency negative feedback, operating between the second and fourth stages, by simply connecting the screens. The low noise required the use of high transconductance tubes in the first stage, but these increased the microphonic pickup. The front-panel view is shown in figure 22.

The noise level of the amplifier naturally depends on the frequency band width (filter) and time constant selected. Figure 23 shows the noise level, determined from the operation of the compensated amplifier with varying time constant M, and filter settings, designated from A to E. The noise level is defined by the root-mean-square voltage fed to the input that produces a root-mean-square output voltage without compensation equal to that produced by the thermal noise with compensation in the absence of an input signal.

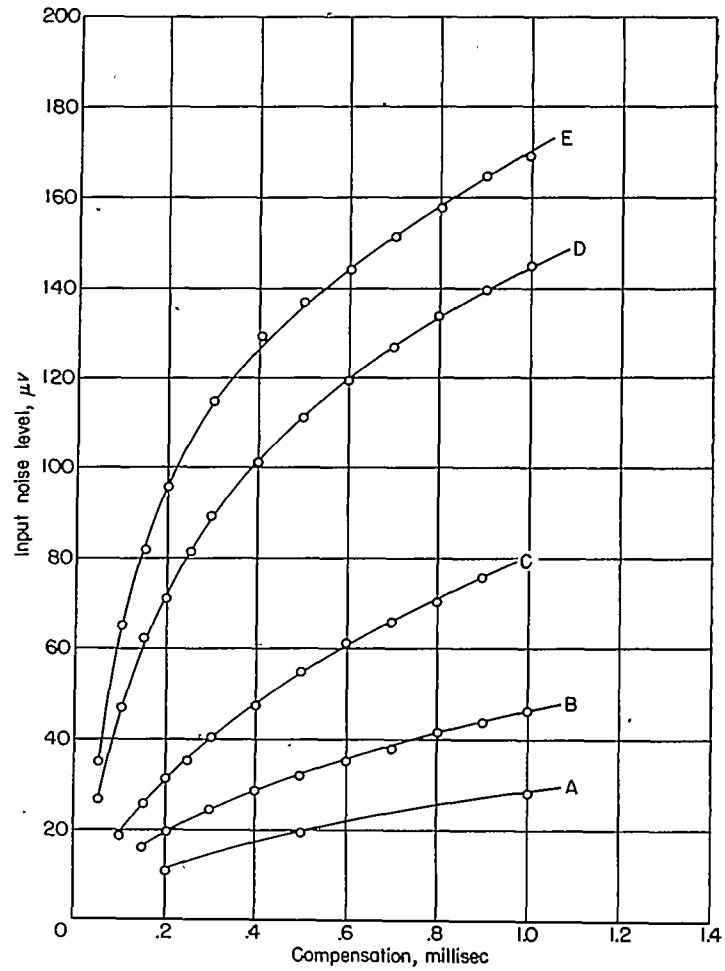

FIGURE 23.—Noise level of compensating amplifier (equivalent input with compensation off).

The problem of frequency-response characteristic adjustment of the amplifier near the upper frequency limit is a matter for compromise. The upper frequency limit affects the noise level and, if only the root-mean-square value of turbulent fluctuations were measured, the ideal frequency response would be uniform up to a given frequency limit, then very sharply cut off. On the other hand, if the phase relations are also important, that is, a faithful response of wave shape is required, then a more "gentle" falling off at high frequencies would be more advantageous. The frequency response may be adjusted by "trimming" the circuit. The frequency response of the amplifier with different cut-off filters in the circuit is shown in figure 24. The amplifier with no low-pass filter has a uniform response approximately up to 160 kilocycles and then falls off gradually. The compensation characteristics for an assumed ideal amplifier are shown in figure 19. The actual compensation characteristics may be obtained by superposition of figures 19 and 24. For low time-constant values the response is limited by the filters; for high time-constant values, by the ceiling-to-floor ratio.

The response of the compensated amplifier may be accurately determined by the method of square waves. A circuit arranged for this purpose is shown in figure 25. Square-wave pulses are fed into a "dummy hot-wire" made up of a decade capacitor and resistance so as to have a time constant in milliseconds equal to the capacitance in microfarads (shunt

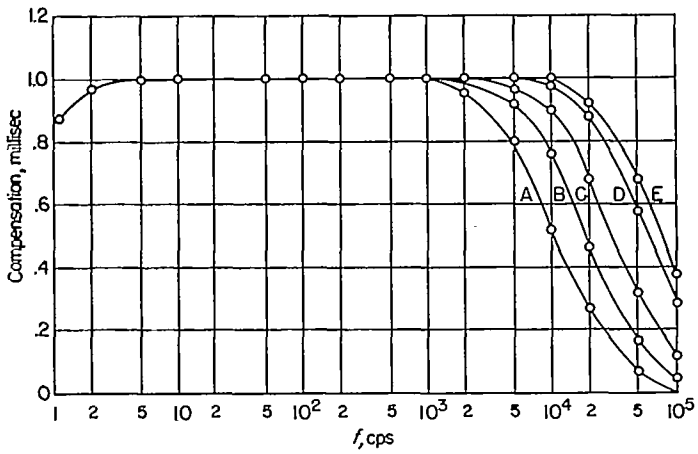

FIGURE 24.—Frequency response of compensating amplifier.

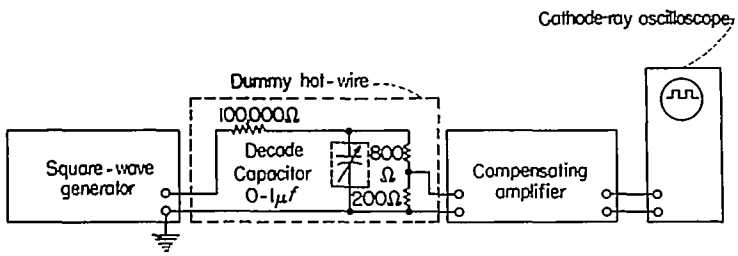

FIGURE 25.—Calibration of compensation performance by square waves.

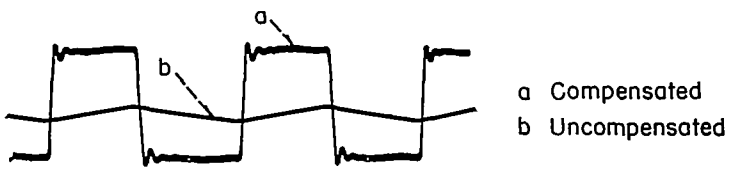

FIGURE 26.—Effect of compensation at high frequency. Time constant, 0.4 millisecond; square-wave frequency, 5,000 cycles per second.

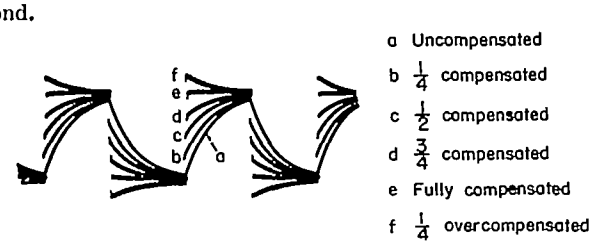

FIGURE 27.—Various degrees of compensation. Time constant, 0.4 millisecond; square-wave frequency, 500 cycles per second.

resistance=1,000 ohms) and a frequency response identical to a real hot-wire with the same time constant. The frequency characteristics at the output of the amplifier are then determined by the wave form appearing on the screen of the cathode-ray oscilloscope. The square-wave input signal distorted to simulate the behavior of the hot-wire is known to be properly compensated when the output signal is restored to its original form. The screen was photographed during a variety of tests and some of the photographs have been reproduced in figures 26 to 29.

Figure 26 shows how much a square-wave signal of 5,000 cycles per second is attenuated by a hot-wire having a time constant of 0.4 millesecond and how the greatly reduced and distorted signal can be restored by compensation. This shows how much information would be lost without compen-

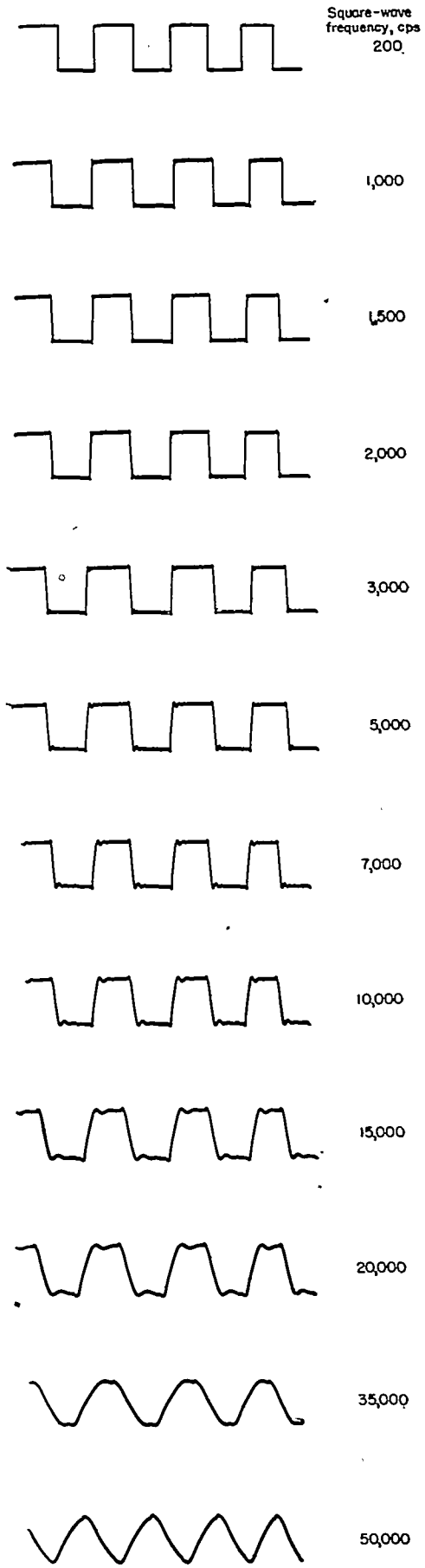

FIGURE 28.—Square-wave response of compensation.

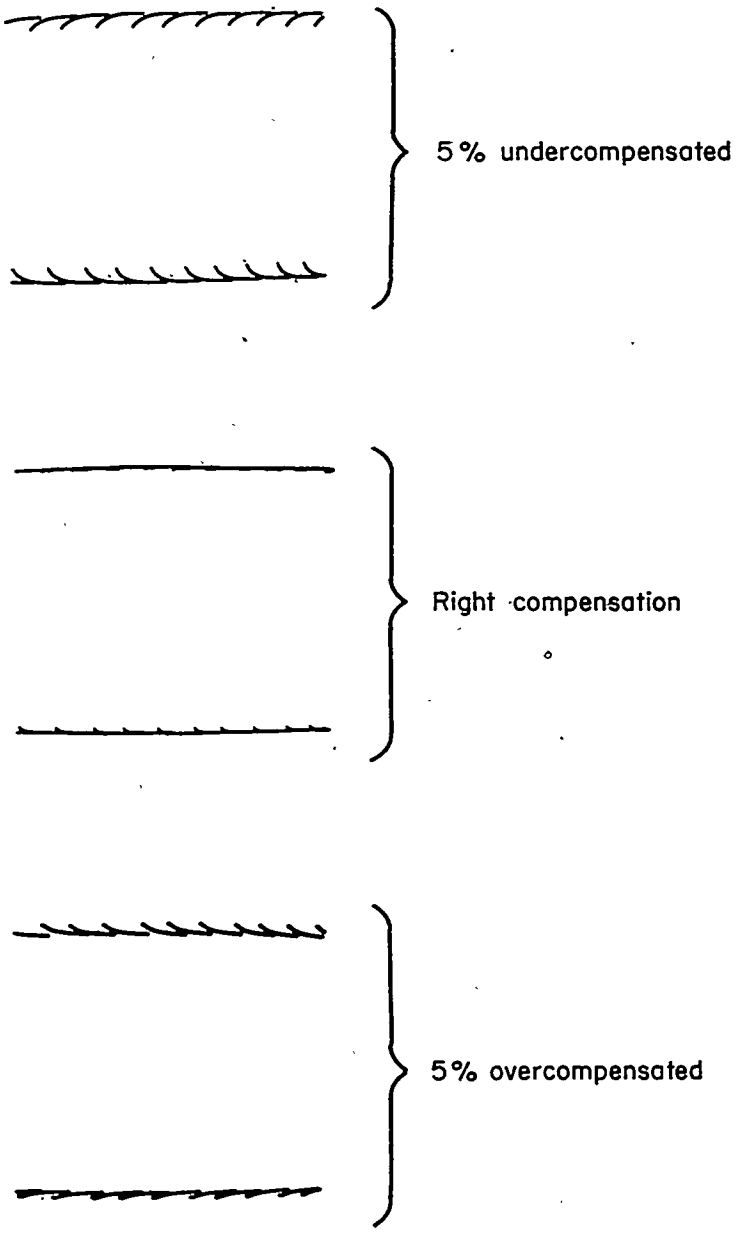

FIGURE 29.—Sensitivity of square-wave method.

sation. Figure 27 shows the patterns obtained by varying the compensation setting. Figure 28 shows the response of the compensated amplifier to square-wave frequencies from 200 to 50,000 cycles per second. The progressive departure from square-wave form shows the continual elimination of higher harmonics. A symmetrical square wave has only odd Fourier components with amplitudes decreasing inversely proportional to their frequency. If only the fundamental frequency passes through the amplifier, the third harmonic is already out of the range. This condition probably has been reached for the 35,000-cycle-per-second square wave and definitely has been reached for 50,000 cycles per second because of the near sinusoidal form at the output. This indicates that full cut-off lies between 105,000 and 150,000 cycles per second. On the other hand, the contribution of the third harmonic is clearly visible in the 20,000-cycle-per-second trace, indicating an appreciable response at 60,000 cycles per second. The 15,000-cycle-per-second signal has an additional contribution from the fifth harmonic. Since higher and higher harmonics come through as the signal frequency decreases, the wave shape becomes more and more square. However, as may be observed from figure 19, the effect of compensation also deteriorates with increased hot-wire time constant.

The method of square waves is very sensitive for compensation setting, especially when the square waves overlap. Figure 29 demonstrates the sensitivity of this method. The slight difference between the upper and lower side of the trace is due to a slight nonlinearity of the scope used.

With a square-wave input and proper compensation for 0.4 millisecond, the rise time of the output wave is approximately 8 microseconds. The rise time here is defined as the time required for the output voltage to rise from 10 to 90 percent of its final value when a discontinuous transient (step-function) voltage is applied to the input. The same definition would give a rise time of 880 microseconds for the uncompensated wave, so the improvement is of the order of 100 depending slightly on the definition.

SERVICE UNIT

If the correlation between two signals is measured by the ratiometer method as described in the section entitled "General Design Considerations," the two outputs from the compensating amplifier must be combined to form the sum and the difference of the two signals. The compensating amplifiers are provided with gain control only in steps; therefore additional continuous amplitude controls are necessary in the service unit. The equality of the root-mean-square level of the two signals necessitates the incorporation of a thermocouple meter.

The circuit diagram is given in figure 30. Two input circuits are provided by small-range amplitude controls and rectifier-type level meters to equalize the signals. The sum and difference of the two signals are produced by a special ring circuit. Outputs are provided by convenient switching. A thermocouple root-mean-square meter circuit is incorporated. The only special feature is the sum-difference circuit. If a ring of eight identical resistors is fed by two independent alternating-current signals at diametrically opposite points, pairs of resistors will connect each pair of feeding points. The midpoint of these pairs of resistors gives the arithmetic mean of the potentials; therefore one pair of diametrical tap points gives the half sum, and the other, the half difference, of the two input voltages (fig. 31).

For calibration purposes it is desirable to feed identical signals to the two systems. This can be achieved by closing the "I=II" switch.

The compensating amplifier must be terminated by a 3,000-ohm load resistor to ground on each side. This resistor is not incorporated in the amplifier unit. The equalizing and metering circuit provides a load of approximately 3,000 ohms on the compensating-amplifier outputs. The front panel is shown in figure 32. Auxiliary circuits have been added to serve other equipment. This fact accounts for the extra features in the photograph.

POWER UNIT

The ratiometer method of measuring correlation requires higher direct-current output from the square detector than

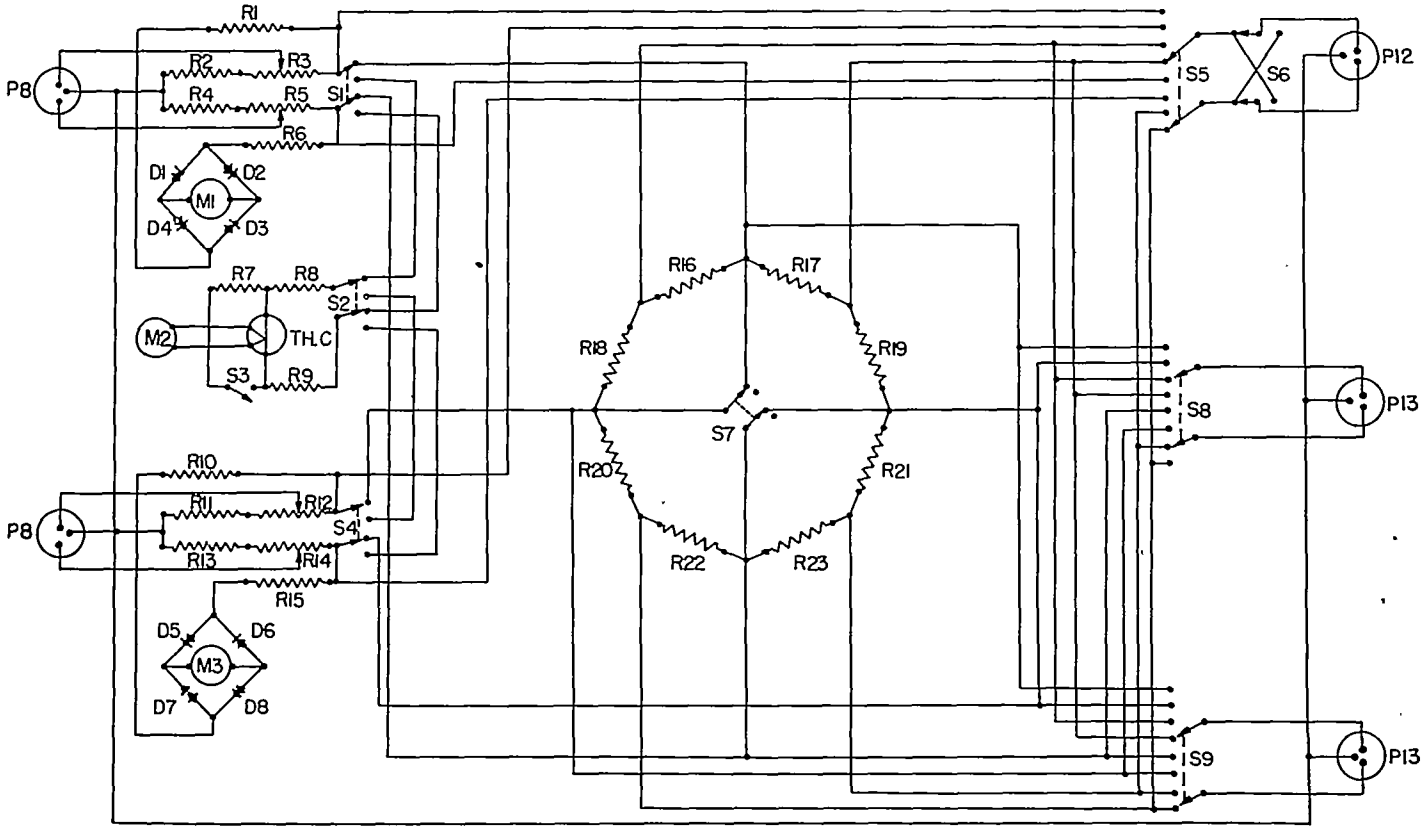

Symbol	Description	Value	Rating	Manufacturer	Type
R1, R6	Resistor, carbon	39,000 Ω±5%	½ w		
R2, R4	Resistor, Carbofilm	4,000 Ω±1%	1 w		
R3, R5	Potentiometer, ganged	1,500 and 1,500 Ω	2 w		
R7	Resistor, Carbofilm	1,000 Ω±1%	1 w		
R8, R9	Resistor, Carbofilm	5,000 Ω±1%	1 w		
R10, R15	Resistor, carbon	39,000 Ω±5%	½ w		
R11, R13	Resistor, Carbofilm	4,000 Ω±1%	1 w		
R12, R14	Potentiometer, ganged	1,500 and 1,500 Ω	2 w		
R16, R23	Resistor, Carbofilm	6,000 Ω±1%	1 w		
M1, M3	Microammeter	0–200 μa		Weston Electrical Instrument Corp	3
M2	Millivoltmeter	0–2 mv		Rowson Electric Co.	
D1 to D8	Germanium diode			Sylvania Electric Products, Inc	1N34
TH. C	Indirectly heated thermocouple	1.5 ma heating for 5 mv output		Am. Thermo Electric Corp.	
S1, S4, S6, S7	Toggle switch, double-pole double-throw.				
S5, S8, S9	Rotary switch	Two poles, five positions.			
S2	Lever-action switch			Centralab Div., Globe-Union, Inc	1454
S3	Telephone-type switch				14S-1P

FIGURE 30.—Service unit.

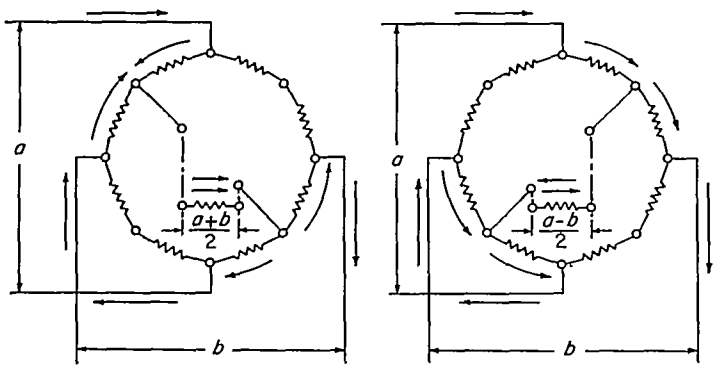

FIGURE 31.—Sum-difference circuit.

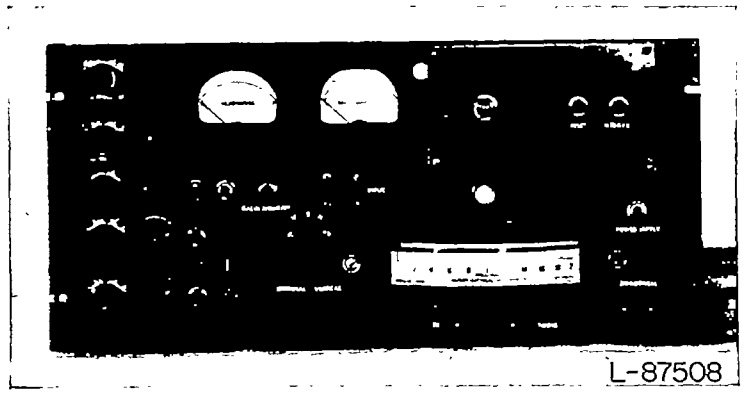

FIGURE 32.—Service unit, front view.

is available from thermocouples. A higher power square detector and also a higher output amplifier have a number of other possible applications (e. g., recording of output level).

The signal level emerging from the compensating amplifier is 1 to 5 volts except under rather special circumstances, for example, taking low-frequency measurements without thermal-lag compensation or making use of the then low noise level (3 to 4 microvolts). In this case the output may be as low as 50 to 100 millivolts. The circuit diagram of the power unit is shown in figure 33. The power unit also incorporates two differentiating circuits that can be cascaded to provide second derivatives with respect to time. Depending on the frequency range, the time constant of the differentiation

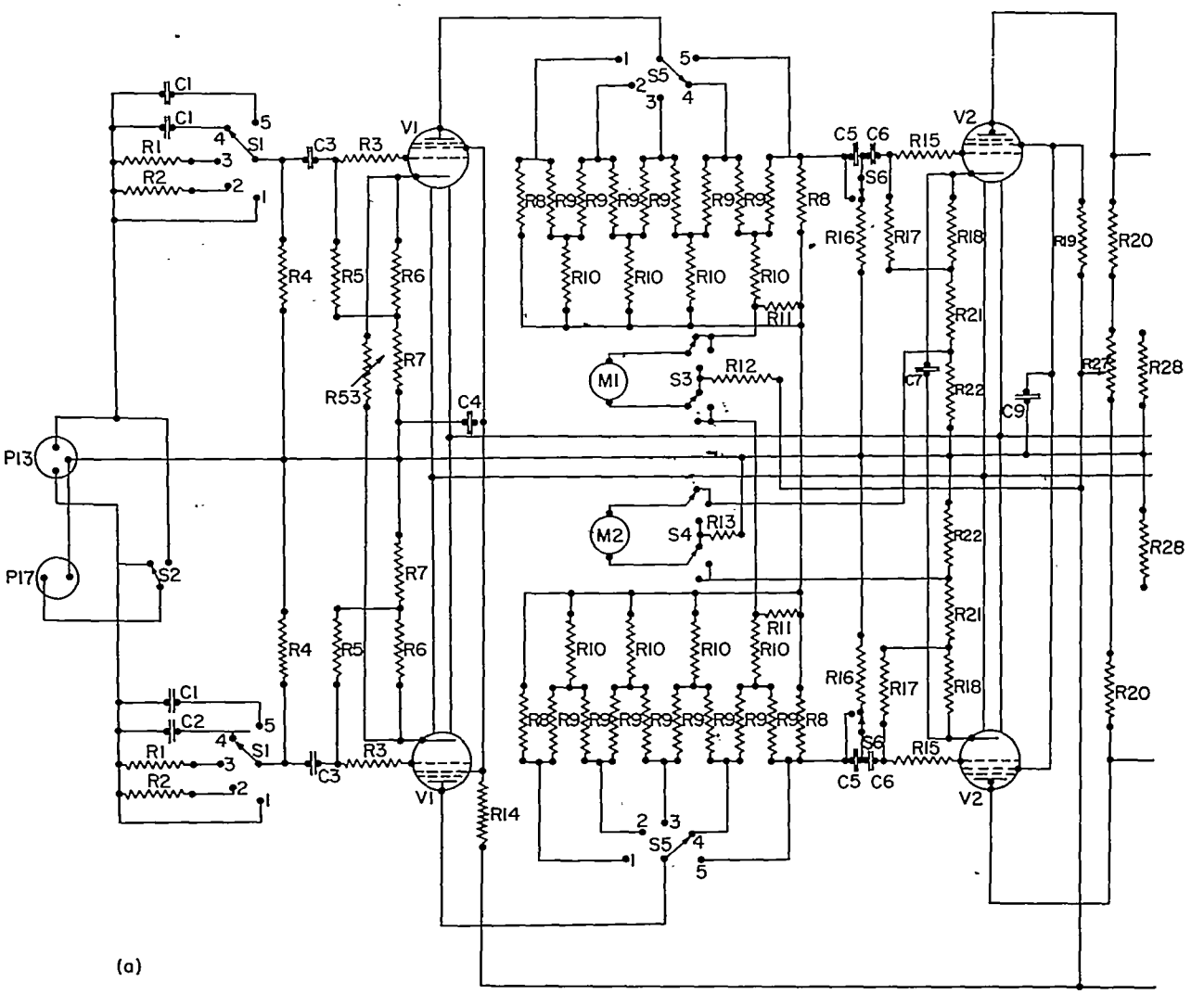

(a)

Symbol	Description	Value	Rating	Manufacturer	Type
V1, V2	Electron tube			Raytheon Mfg. Co.	CK 5654
V3	Electron tube			Raytheon Mfg. Co.	6AS7
V4 to V14	Electron tube			Raytheon Mfg. Co.	6AL5
V15, V18	Electron tube			Raytheon Mfg. Co.	OB2
V16	Electron tube			Raytheon Mfg. Co.	OA2
V17	Electron tube			Raytheon Mfg. Co.	5V4
TR	Power transformer	115 v primary, 2×500 v secondary		United Transformer Corp.	OG-431
L1	Filter choke	10 h at 60 ma; d-c resistance, 275 Ω		The Halldorson Co.	B4-839
L2, L3	Filter choke	15 h at 200 ma; d-c resistance, 150 Ω		The Halldorson Co.	S-240
L4, L5	Filter choke	10 h at 0 ma; 7 h at 300 ma d. c., d-c resistance, 60Ω	Max. current, 375 ma	Thordarson Elec. Mfg. Div., Maguire Inds., Inc.	T20C56
C1	Capacitor	0.005 μf	600 v	Electro-Motive Mfg. Co., Inc.	Elmenco mica
C2	Capacitor	0.001 μf	600 v	Electro-Motive Mfg. Co., Inc.	Elmenco mica
C3	Capacitor, oil-filled	0.5 μf	600 v	Cornell-Dubilier Elec. Corp.	Bath tube
C4	Capacitor, electrolytic	10 μf	450 v	Aerovox Corp.	Can
C5	Capacitor	0.003 μf	600 v	Electro-Motive Mfg. Co., Inc.	Elmenco mica
C6	Capacitor, oil-filled	0.5 μf	600 v	Cornell-Dubilier Elec. Corp.	Bath tube
C7	Capacitor, variable	0.0005 μf			Trimmer
C8	Capacitor	0.5 μf	600 v	Cornell-Dubilier Elec. Corp.	Bath tube
C9	Capacitor, electrolytic	10 μf	450 v	Aerovox Corp.	Can
C10, C11	Capacitor, electrolytic	40 μf	450 v		
C12	Capacitor, electrolytic	80 μf	500 v		Can
C13	Capacitor, electrolytic	80 μf	500 v		Can
C14	Capacitor, electrolytic	80 μf	500 v		Can
C15, C16	Capacitor, electrolytic	40 μf	450 v		Can
C17	Capacitor, electrolytic	500 μf	10 v		
R1	Resistor, Carbofilm	100,000 Ω±5%	1 w		
R2	Resistor, Carbofilm	20,000 Ω±5%	1 w		
R3	Resistor, Carbofilm	1,000 Ω±1%	½ w		
R4	Resistor, Carbofilm	5,000 Ω±1%	½ w		
R5	Resistor, Carbofilm	500,000 Ω±1%	½ w		
R6	Resistor, Carbofilm	200,000 Ω±1%	½ w		
R7	Resistor, Carbofilm	2,000 Ω±1%	1 w		
R8	Resistor, wirewound	8,750 Ω±1%	1 w	Western Elec. Co., Inc.	
R9	Resistor, wirewound	1,500 Ω±1%	1 w	Western Elec. Co., Inc.	
R10	Resistor, wirewound	25,000 Ω±1%	1 w	Western Elec. Co., Inc.	
R11	Resistor, Carbofilm	200 Ω±1%	1 w		
R12, R13	Resistor, Carbofilm	3,000 Ω±1%	1 w		
R14	Resistor, Carbofilm	30,000 Ω±1%	1 w		
R15	Resistor, Carbofilm	1,000 Ω±1%	½ w		
R16	Resistor, Carbofilm	10,000 Ω±1%	½ w		
R17	Resistor, Carbofilm	500,000 Ω±1%	½ w		
R18	Resistor, Carbofilm	200 Ω±1%	½ w		
R19	Resistor, Carbofilm	50,000 Ω±5%	1 w		
R20	Resistor, Carbofilm	20,000 Ω±1%	1 w		
R21	Resistor, Carbofilm	2,000 Ω±1%	1 w		
R22	Resistor, carbon	200 Ω±5%	½ w		
R23	Resistor, Carbofilm	1,000 Ω±1%	½ w		
R24	Resistor, Carbofilm	500,000 Ω±1%	½ w		
R25	Resistor, Carbofilm	50,000 Ω±1%	1 w		
R26	Resistor, wirewound	5,000 Ω±1%	5 w		
R27	Potentiometer, wirewound	10,000 Ω	2 w	Mallory Elec. Corp.	Linear M10MP
R28	Resistor, Carbofilm	100,000 Ω±1%	1 w		
R29	Potentiometer, carbon	100,000 Ω	2 w		

FIGURE 33.—Power unit.

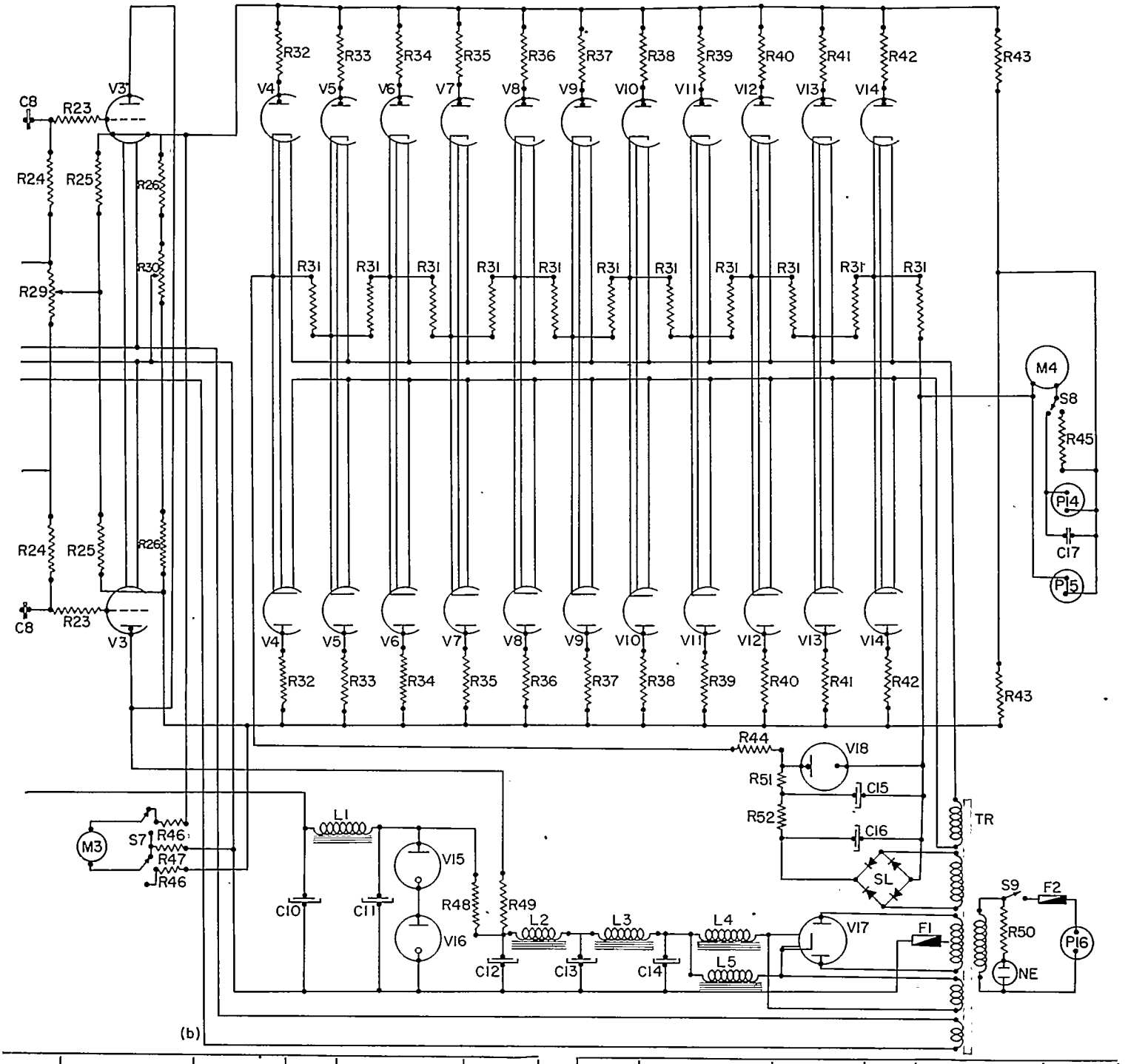

Symbol	Description	Value	Rating	Manufacturer	Type
R30	Potentiometer, wirewound	1,000 Ω	2 w	Mallory Elec. Corp.	M1MP
R31	Resistor, carbon	220±1%	½ w		
R32	Resistor, Carbofilm	3,900 Ω±1%	½ w		
R33	Resistor, Carbofilm	7,300 Ω±1%	½ w		
R34	Resistor, Carbofilm	11,100 Ω±1%	½ w		
R35	Resistor, Carbofilm	15,600 Ω±1%	½ w		
R36	Resistor, Carbofilm	20,800 Ω±1%	½ w		
R37	Resistor, Carbofilm	26,200 Ω±1%	½ w		
R38	Resistor, Carbofilm	31,900 Ω±1%	½ w		
R39	Resistor, Carbofilm	37,800 Ω±1%	½ w		
R40	Resistor, Carbofilm	45,000 Ω±1%	½ w		
R41	Resistor, Carbofilm	53,200 Ω±1%	½ w		
R42	Resistor, Carbofilm	60,400 Ω±1%	½ w		
R43	Resistor, wirewound	2,000 Ω±1%	5 w		
R44	Resistor, wirewound	1,500 Ω	10 w		
R45	Resistor, Carbofilm	1,220 Ω±1%	1 w		
R46	Resistor, carbon	220,000 Ω±5%	½ w		
R47	Resistor, carbon	4,400,000 Ω±5%	1 w		
R48	Resistor, wirewound	2,000 Ω±5%	10 w		
R49	Resistor, wirewound	100 Ω±5%	5 w		

Symbol	Description	Value	Rating	Manufacturer	Type
R50	Resistor, carbon	220,000 Ω±10%	½ w		
R51	Resistor, wirewound	200 Ω	5 w		
R52	Resister, wirewound	1,000 Ω	5 w		
R53	Potentiometer, wirewound	500 Ω	2 w	Mallory Elec. Corp.	
SL	Selenium rectifier	130 v	75 ma	Federal Elec. Products Co.	#1003
F1	Fuse		0.5 amp		AGC
F2	Fuse		5 amp		AGC
NE	Neon indicating bulb		⅛5 w	General Elec. Co.	E51
S1, S5	3-circuit 5-position switch			Centralab Div., Globe-Union, Inc.	V 9002
S2, S6, S8, S9	Double-pole double-throw switch.				
S3, S4, S7	Lever-action switch			Centralab Div., Globe-Union, Inc.	1454
M1, M2, M3	Microammeter	50, 0, 50 μa	Resist 1,010	Int. Instrs. Inc.	Model 15
M4	Microammeter	0, 500 μa	Resist 100	Sensitive Res. Instr. Corp.	Model UP

FIGURE 33.—Concluded.

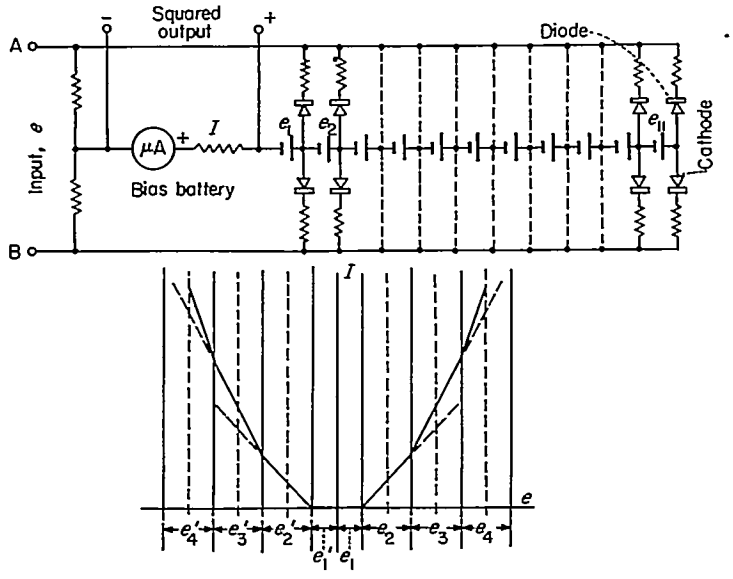

FIGURE 34.—Biased-diode square-law detector.

circuit can be varied by changing the capacitor. An attenuator with steps and $1:\sqrt{2}$ ratio controls the gain and a continuous gain control is provided to adjust levels of relative amplification in the two channels (two power units). After two stages of voltage amplification a high-power push-pull stage raises the signal to the 30- to 40-volt level across a rather low impedance (4,000 ohms cathode to cathode). This power is available as an output for any meter or equipment requiring high alternating-current power.

The square detector is a separate circuit within the power unit. Figure 34 shows the square-law detector circuit. The original equipment was built with germanium diodes and small dry-cell batteries for bias. In the new equipment, vacuum-tube diodes are used and the bias is provided as voltage drop through resistors fed from a separate floating power supply. The original circuit is given in figure 34, since it is easier to follow the principle of operation. The circuit uses the biased-diode method that can be adjusted to any monotonic functional relationship between voltage and current. The circuit consists of pairs of rectifiers with series resistors acting as full-wave rectifiers. The bias voltage prevents the rectifiers from conducting before the signal overcomes the bias voltage. Thus with increasing instantaneous voltage more and more stages of rectifier pairs are conducting. The curve of rectified current against input voltage is controlled by the series resistors.

The computation of the circuit can be simplified by assuming continuously distributed rectifying elements and series resistors. If the voltage drop across the meter can be neglected, identical series resistors would produce an exact square law. In the general case the voltage drop across the meter must be subtracted from the input voltage. The following quantities are defined:

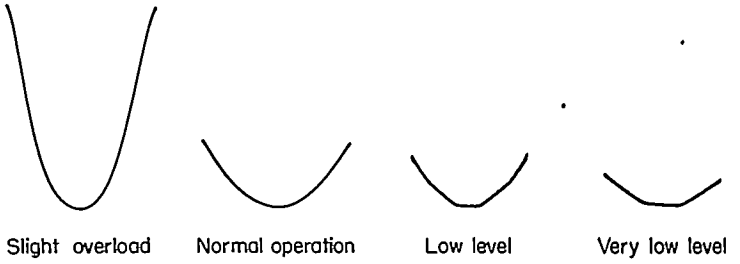

FIGURE 35.—Amplitude response of square-law circuit. Amplification readjusted for each oscillograph. Frequency, 100 cycles per second.

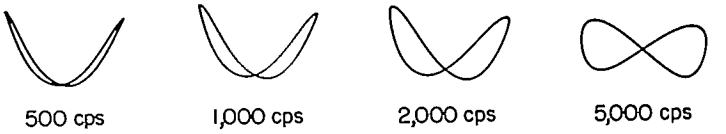

FIGURE 36.—Frequency response of square-law circuit.

e input voltage
I output current
R_m meter resistance
e' input voltage to diode circuit, $e-IR_m$
R_e' value of the resistor in stage that just starts conducting at voltage e'
ΔV bias voltage step between stages

Assuming continuous distribution it can be shown that

$$\frac{d^2I}{(de')^2}=\frac{1}{\Delta V}\frac{1}{R_e'} \tag{31}$$

By choosing the resistors on the basis of this approximate theory the square law established itself remarkably well.

The square-law circuit responds instantaneously within the limitations of capacity effects in the diodes. If the output voltage is plotted against the input voltage (sine-waves input), the resulting Lissajous figure on the cathode-ray oscilloscope is a parabola. Figure 35 shows a series of such parabolas at varying amplitude levels. At low levels the steps are clearly seen, but at higher levels the parabola is practically continuous. The variation of square response with frequency is shown in figure 36. The increasing phase lag produces an ∞-shaped pattern when the phase lag becomes 90°. The quantitative response of the squaring circuit is given in figure 37, showing that the performance is not inferior to that of a thermocouple but produces a substantially higher direct-current output. The front panel arrangement is shown in figure 38. The compact unit of the square-wave detector is shown in figure 39.

CALIBRATION UNIT

The control unit and compensating amplifier have been made in two identical units to provide for two identical channels. The functions that are not needed in duplicate and involve the low signal levels of the amplifier input are

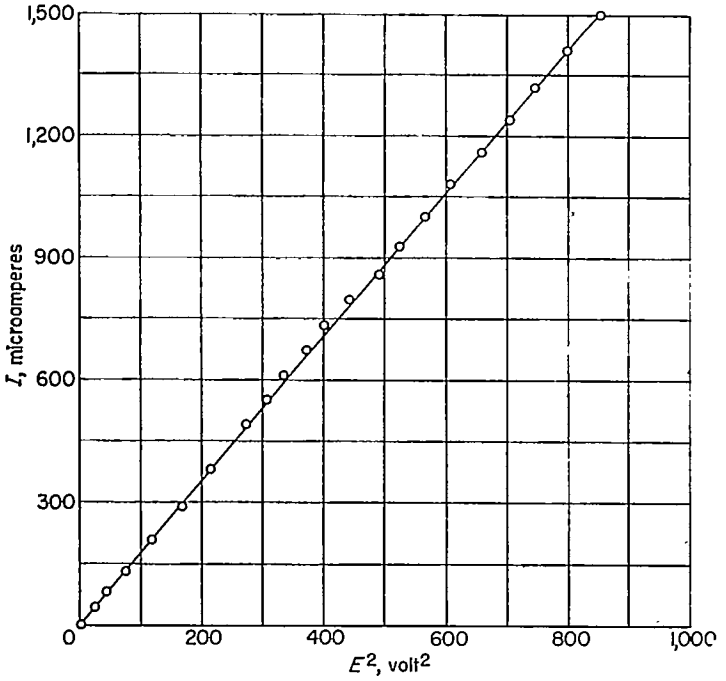

FIGURE 37.—Calibration of square-law circuit.

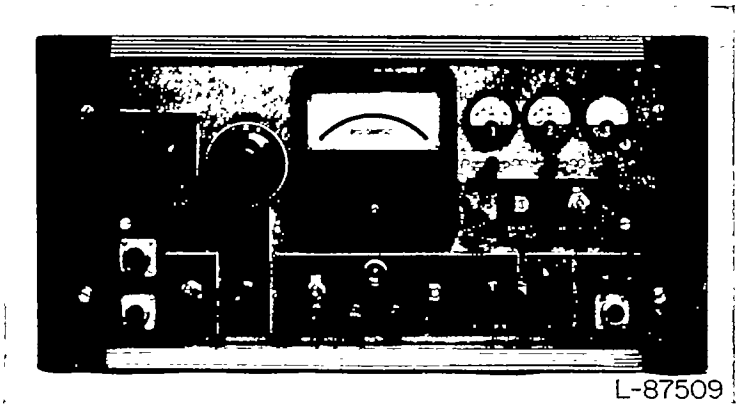

FIGURE 38.—Power unit, front view.

integrated into a calibration unit.

The circuit diagram is given in figure 40 and the front panel is shown in figure 41. There are two independent circuits. One is a calibrating-test voltage supply and the other, a direct-current potentiometer.

The calibrating-test voltage is obtained from an external generator (sine-wave, square-wave, or random-noise). A thermocouple root-mean-square meter (0- to 3-milliampere range) measures the current through the calibrated resistors. A shunt can change the range by a factor of 10. The potential across accurate resistors can give continuous range of test voltages from 300 microvolts to 90 millivolts at any wave form. A "dummy hot-wire" (essentially the same as in fig. 25) is incorporated giving a fixed time constant of 0.5 millisecond.

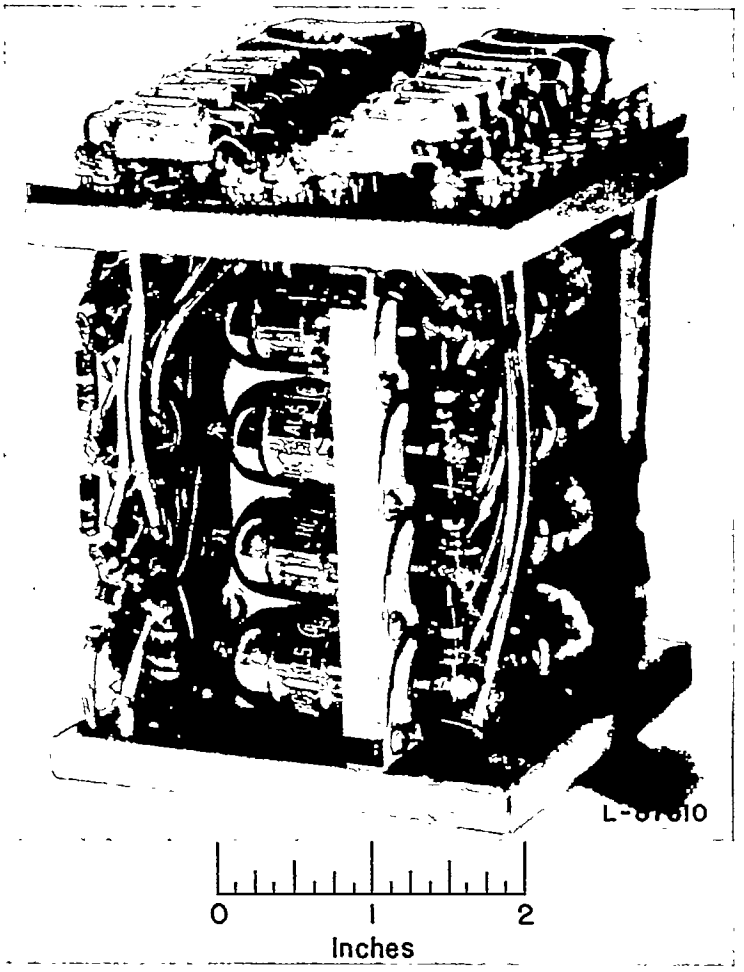

FIGURE 39.—Biased-diode square-law detector in power unit.

AUXILIARY EQUIPMENT

The auxiliary equipment employed is shown dotted in figure 9.

Power supplies.—The compensating amplifiers are supplied with the appropriate forms of power which are controlled and metered. The control units have two power supplies, one for the plate and one for the filament.

Oscilloscope.—An oscilloscope is used to monitor the output signal. The faithful response of the oscilloscope is important in square-wave calibration.

Ratiometer.—It was stated in the section entitled "General Design Considerations" that the ratio of the output currents supplied by the power units can be made a unique function of the correlation coefficient. The ratiometer used was made by the Sensitive Research Co. The power required to operate this instrument is a 0.5-milliampere direct current across a 1,500-ohm resistor, which would produce a 750-millivolt potential drop. The power unit has this capability available, whereas the thermocouples installed in the service unit are incapable of supplying this amount of power.

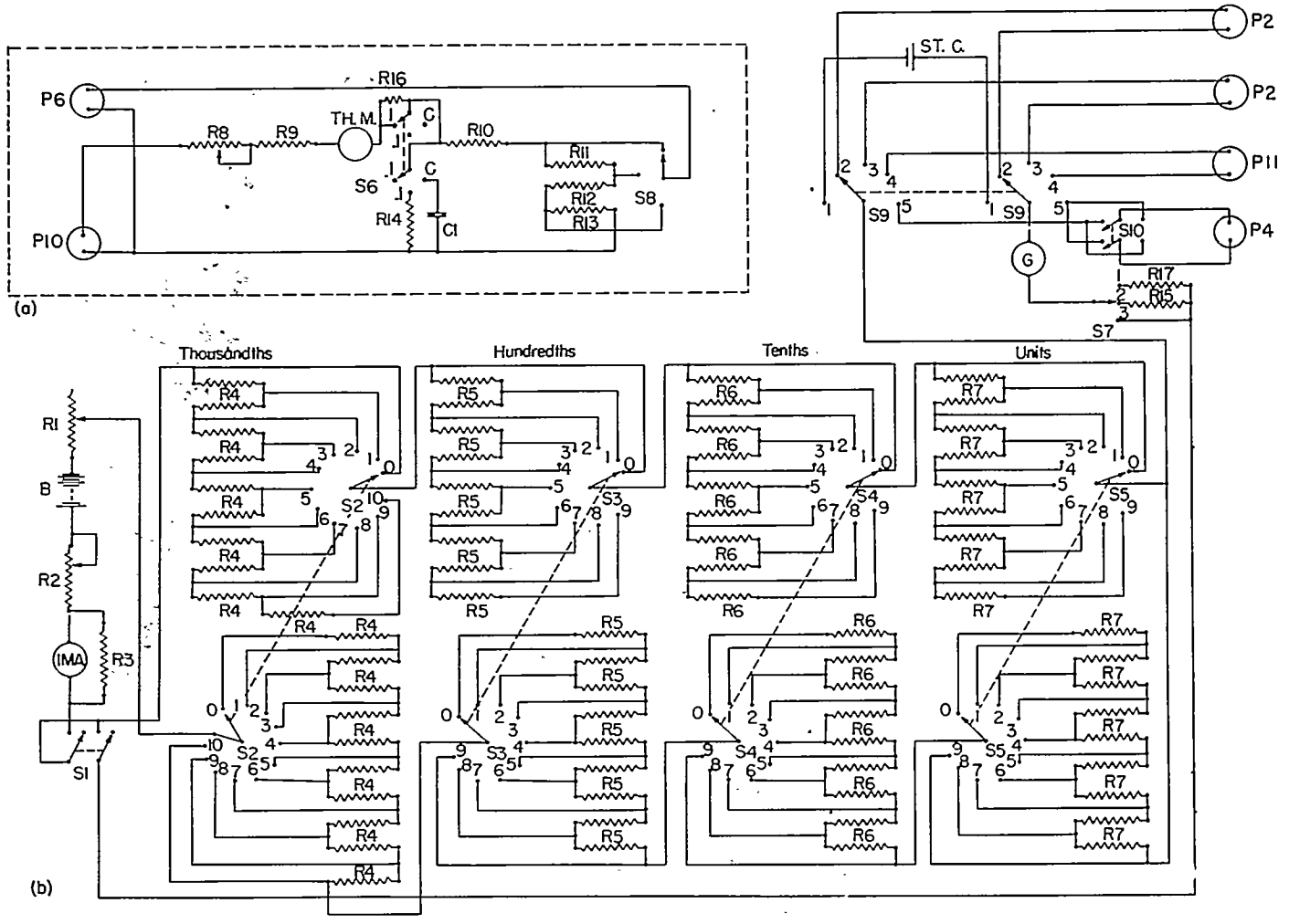

(a) Test-signal calibration.
(b) Direct-current potentiometer.

Symbol	Description	Value	Rating	Manufacturer	Type	Remarks
R1	Center-tap potentiometer, linear wire-wound.	10,000 Ω	4 w	Mallory Electric Corp	M10MP	
R2	Center-tap potentiometer, linear wire-wound.	75 Ω	4 w	Mallory Electric Corp	M75P	
R3	Resistor, Carbofilm	10 Ω	1 w			
R4	Resistor, wire-wound	0.1 Ω±0.1%		The Daven Co	1870A	
R5	Resistor, wire-wound	1 Ω±0.05%		The Daven Co	1871B	
R6	Resistor, wire-wound	10Ω±0.05%		The Daven Co	1871C	
R7	Resistor, wire-wound	100 Ω±0.05%		The Daven Co	1871D	
R8	Center-tap potentiometer, wire-wound.	5,000 Ω	4 w	Mallory Electric Corp	M5MP	
R9	Resistor, Carbofilm	1,000 Ω±1%	1 w			
R10	Resistor, Carbofilm	970 Ω±1%	1 w			
R11	Resistor, Carbofilm	20 Ω±1%	1 w			
R12	Resistor, Carbofilm	7 Ω±1%	1 w			
R13	Resistor, Carbofilm	3 Ω±1%	1 w			
R14	Resistor, Carbofilm	111 Ω±1%	1 w			
R15	Resistor	100,000 Ω	1 w			
R16	Resistor	1,000 Ω	½ w			
R17	Resistor	5,000 Ω	½ w			
C1	Capacitor, mica	0.5 μf±1%		General Radio Co	505X	
S1, S10	Toggle switch, double-pole double-throw.					
S2	Decade potentiometer switch, 0 to 10 positions.			The Daven Co	1870A	Supplied complete with resistors R^4 mentioned above.
S3	Decade potentiometer switch, 0 to 9 positions.			The Daven Co	1871B	Supplied complete with resistors R^5 mentioned above.
S4	Decade potentiometer switch, 0 to 9 positions.			The Daven Co	1871C	Supplied complete with resistors R^6 mentioned above.
S5	Decade potentiometer switch, 0 to 9 positions.			The Daven Co	1871D	Supplied complete with resistors R^7 mentioned above.
S6, S8	Lever-action switch	2 poles, 3 positions		Centralab Div., Globe-Union, Inc	1454	
S7	Telephone-key switch.					
S9	Rotary switch.	2 poles, 5 positions				
G	Galvanometer	15–0–15 μa±1%		Sensitive Research Instrument Corp	yW	100-Ω internal resistance
IMA	Milliameter	1ma±2%		Weston Electrical Instrument Co	301	3 in.
TH. M	Milliameter, radio-frequency	0–3 ma±2%		Weston Electrical Instrument Co	425	Specially ordered
B	Battery	15 v		Radio Corp. of Am	Flashlight	Normal

FIGURE 40.—Calibration unit.

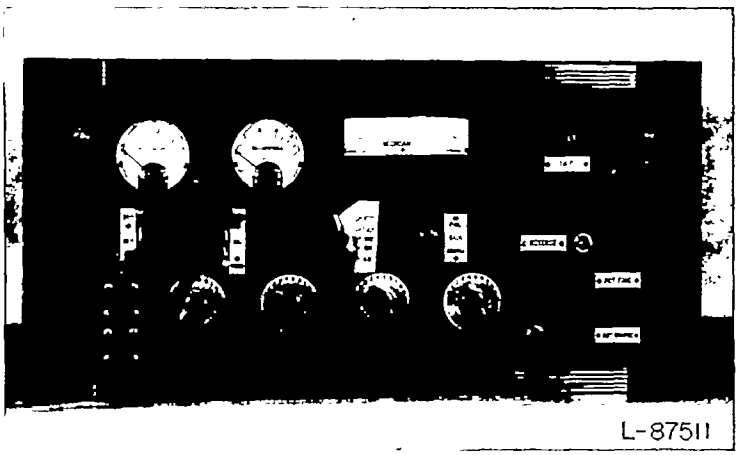

FIGURE 41.—Calibration unit, front view.

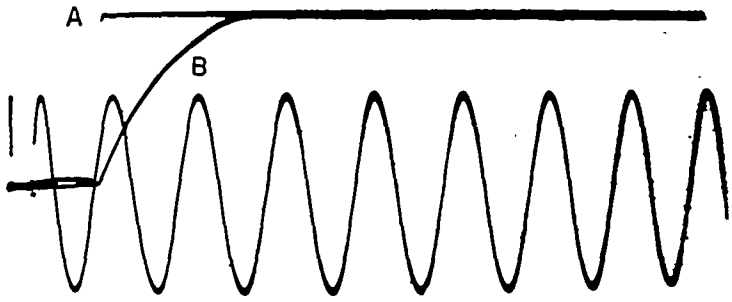

FIGURE 42.—Hot-wire response to traveling shock wave. Compensated A and uncompensated B record from shock wave. Wollaston wire, diameter, 0.0001 inch; heating current, 21.42 milliamperes; $a_r'=0.47$; time constant $M=0.225$ millisecond; calibrating sine wave, 5-kilocycle, 75-millivolt root-mean-square value.

Wave analyzer.—A narrow-band-width wave analyzer is used to measure the power contribution to the total signal by the different frequency bands. The commercially available equipment is designed primarily to isolate discrete spectral lines and is calibrated accordingly. Some modifications, such as the use of a square detector for output meter, are necessary to measure the proper quantities.

SAMPLE MEASUREMENTS

A few sample experimental results are submitted. This has been done not so much for the information contained but to demonstrate the soundness in design principle of the equipment by its performance in the manner expected.

TIME RECORD OF HOT-WIRE OUTPUT IN A SHOCK TUBE

When a traveling shock wave passes by a point in a shock tube, the density and absolute temperature increase discontinuously and the velocity rises abruptly from zero to a finite value. If a hot-wire probe is inserted into the shock tube, a transient change occurs in the flow conditions during a period that is extremely short compared with the response time of the wire and accompanying apparatus. In accordance with the theory, the uncompensated wave shape should still be exponential, even though the simple linearized thermal-lag equation is not applicable. Figure 42 shows an uncompensated and a compensated record together with a

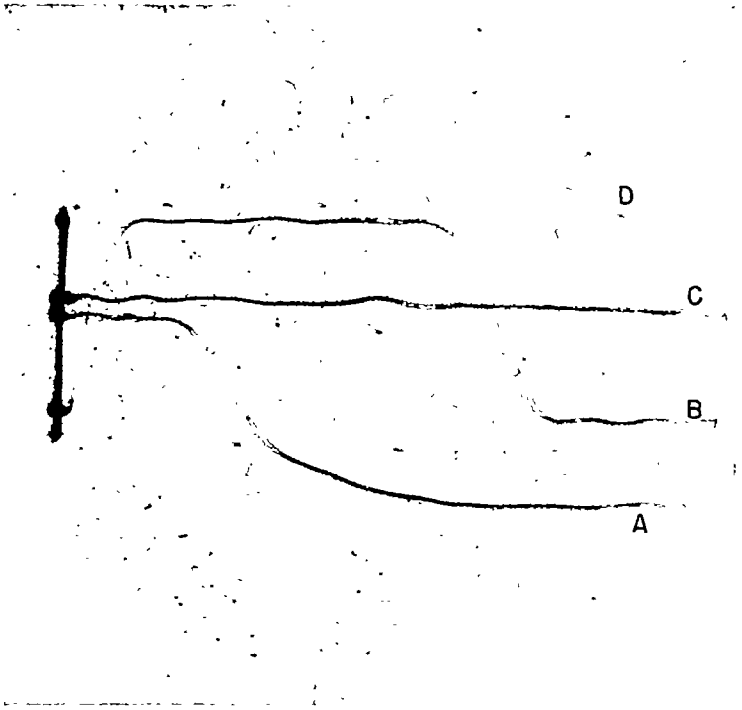

FIGURE 43.—Ultimate resolution of hot-wire method. A, shock-wave record, compensated; B, 10-kilocycle square-wave record, compensated; C, no signal; D, sine wave, 50-kilocycle, 75-millivolt root-mean-square value. Shock-wave indication rises sharply, then becomes less steep, probably because shock reflection from wedge-shaped holder becomes significant. $R_w=33.3$ ohms; $I=13.56$ milliamperes; time constant $M=0.205$ millisecond.

5,000-cycle-per-second sine wave. The records prove that with compensation high fidelity has been achieved. Oscillograph records obtained at a higher writing speed more completely resolve the details of the transient response performance, and, in the presence of a timing signal, the rise time can be estimated. Figure 43 shows three traces illustrating the transient response of the wire to a step function in flow conditions (A) and in heating current (B). The rise time measured is of the order of 10 to 15 microseconds. This work was carried out in the Department of Aeronautics at The Johns Hopkins University.

MASS-FLOW AND STAGNATION-TEMPERATURE FLUCTUATIONS IN A SUPERSONIC TUNNEL

A 0.00015-inch-diameter tungsten wire of approximately 0.080-inch length was used in this investigation. The sensitivity of the wire is given in figure 8. The instantaneous voltage fluctuation across the wire is given in equation (15). The mean-square voltage fluctuation

$$\overline{(\Delta e')^2}=\overline{\Delta e^2}=\Delta e_m{}^2\overline{(m')^2}+\Delta e_T{}^2\overline{(\vartheta)^2}-2\Delta e_m\,\Delta e_T\overline{m'\vartheta}R_{mT} \qquad (32)$$

with

$$m'=100\,\frac{\sqrt{\overline{\Delta(\rho U)^2}}}{\bar{\rho}\,\bar{U}}$$

$$\vartheta=100\,\frac{\sqrt{\overline{(\Delta T_o)^2}}}{\overline{T_o}}$$

$$R_{mT}=\frac{\overline{\Delta(\rho U)\,\Delta T_o}}{\sqrt{\overline{\Delta(\rho U)^2}}\sqrt{\Delta T_o^2}}$$

If the correlation between mass-flow fluctuations and stagnation-temperature fluctuation is complete ($R_{mT}=\pm 1$), the plot of

$$\frac{\Delta e'}{\Delta e_T}=f\left(\frac{\Delta e_m}{\Delta e_T}\right)$$

must be a linear one. The intersection at

$$\frac{\Delta e_m}{\Delta e_T}=0$$

equals ϑ and the slope is m' for $R_{mT}=-1$ or $-m'$ for $R_{mT}=1$.

A tungsten wire 0.00015 inch in diameter and approximately 0.08 inch long was exposed to an air stream with $M=1.73$ and a supply pressure of 40 centimeters of mercury. The sensitivity for mass-flow fluctuations varied by 1 to 10 millivolts per percent and the sensitivity for stagnation-temperature fluctuation varied by 3 to 10 millivolts per percent corresponding to 1 millivolt to 3 millivolts per °C. The ratio of sensitivities varied by a factor of 1 to 15 in the

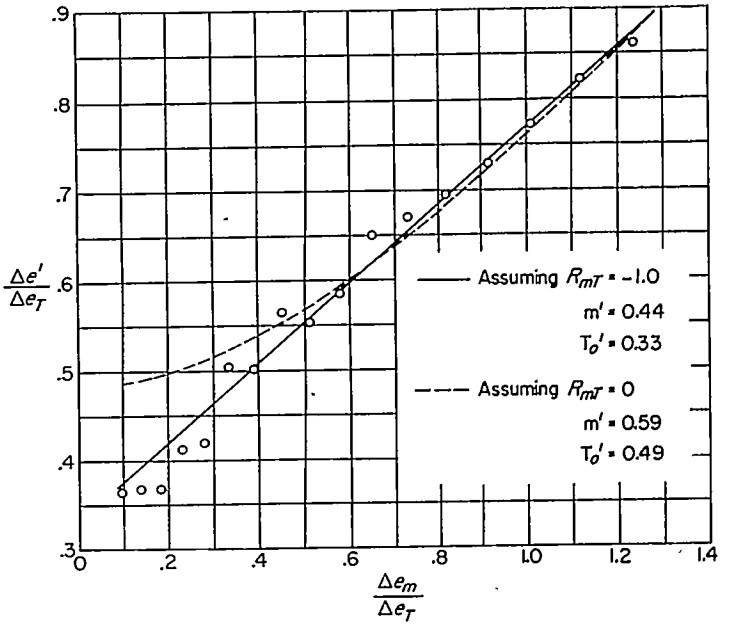

FIGURE 44.—Graphical separation of mass-flow and temperature fluctuations.

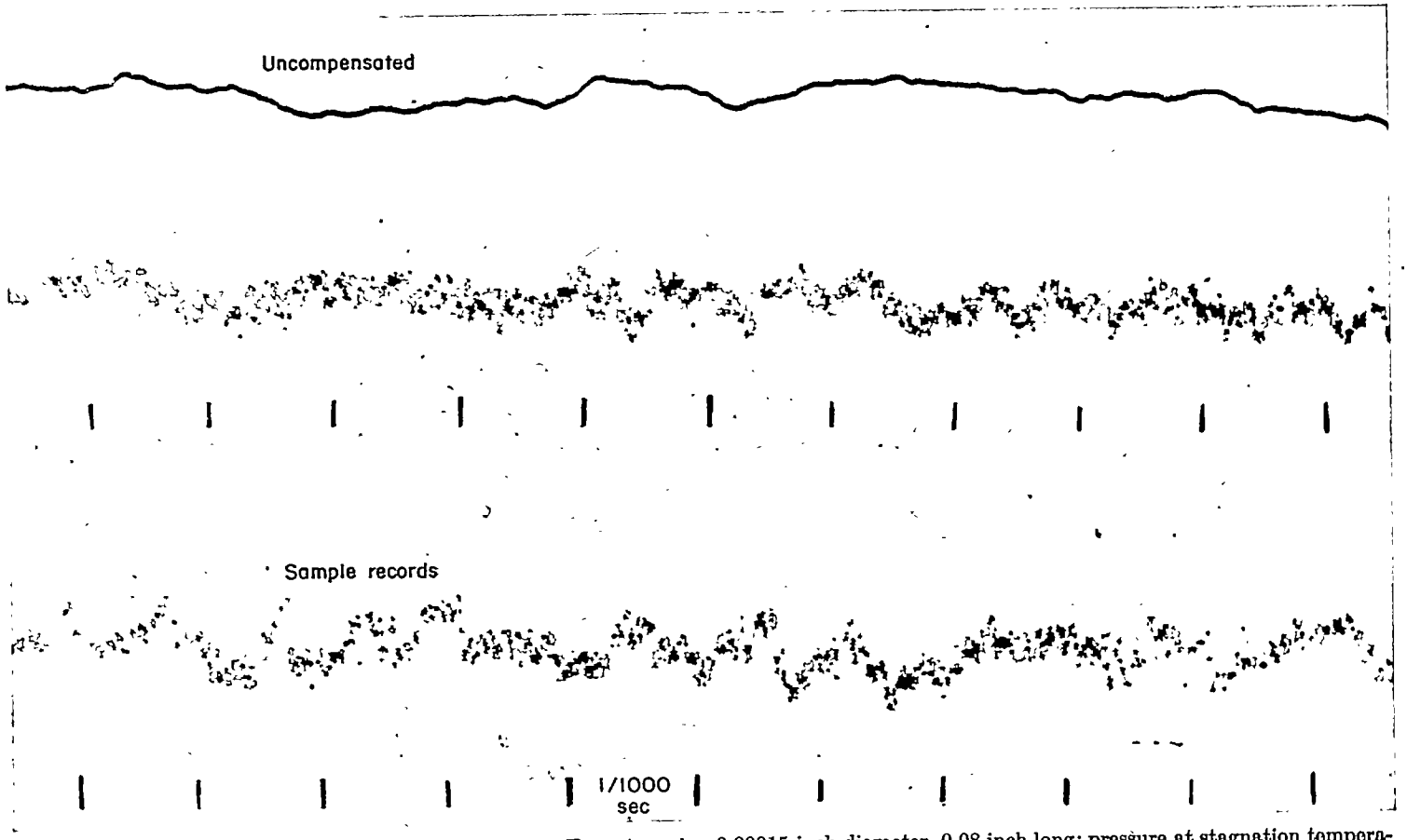

FIGURE 45.—Hot-wire record in supersonic wind tunnel. Tungsten wire, 0.00015-inch diameter, 0.08 inch long; pressure at stagnation temperature, 40 centimeters of mercury; T_o=16° C (289° K); Mach number, 1.73; current, 46.2 milliamperes; T_w=101° C (374°K); R_w=13.4 ohms; time constant M=0.45 millisecond.

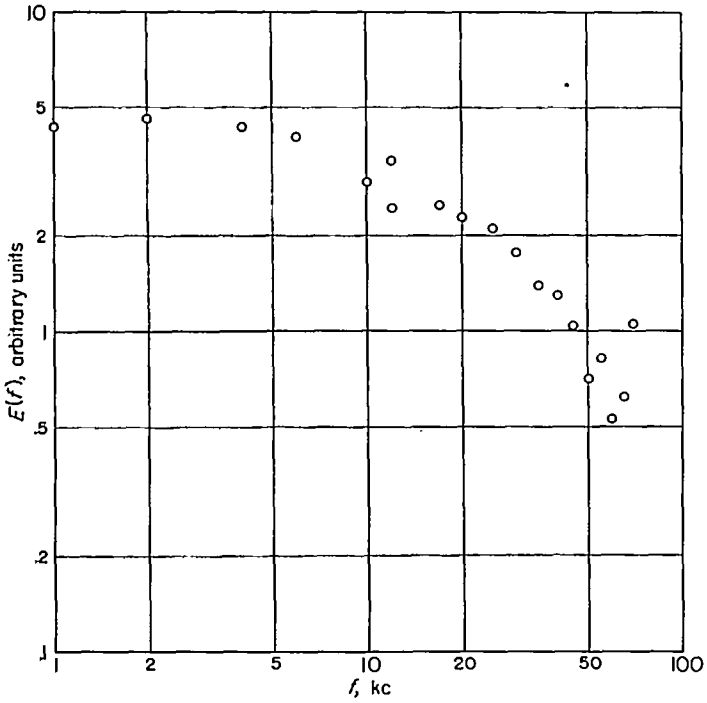

FIGURE 46.—Power spectrum of turbulent fluctuations in supersonic boundary layer. Free-stream Mach number, 1.75; atmospheric pressure; stagnation temperature T_0=20° C (293° K); boundary-layer thickness, 0.500 inch; probe location y= 0.250 inch.

useful range. Figure 44 shows a plot of the separation of mass-flow and temperature fluctuations obtained in the Aberdeen Bomb Tunnel when the turbulence was artificially increased in the settling chamber. The graph suggests strongly that R_{mT}=−1 in this case. Later analysis of the same data (fig. 10 in ref. 3) indicates that the fluctuations were primarily "temperature spottiness" or "entropy mode."

An oscillographic record taken during the same experiment is shown in figure 45. Note the high-frequency content of the hot-wire output. This is not the random noise produced by the equipment since the signal-to-noise ratio was approximately 30:1 (in power). The energy spectrum was measured by a specially built superheterodyne wave analyzer up to 70 kilocycles. A supersonic boundary layer about 0.5 inch thick was explored (ref. 3) and the spectrum found is shown in figure 46. The noise level is about one-sixth of the signal at the upper end.

TURBULENCE SPECTRUM IN LOW-SPEED FLOW

The performance of the turbulence-measuring equipment described in this report seems to be superior to that of previously reported instruments at both high and low speeds. Figure 47 shows an energy-spectrum measurement in a turbulent boundary layer. The noise and the turbulent-velocity fluctuation are both random functions. The energy spectrum of the signal decreases with rising frequency. The spectrum of the amplifier noise is flat without compensation,

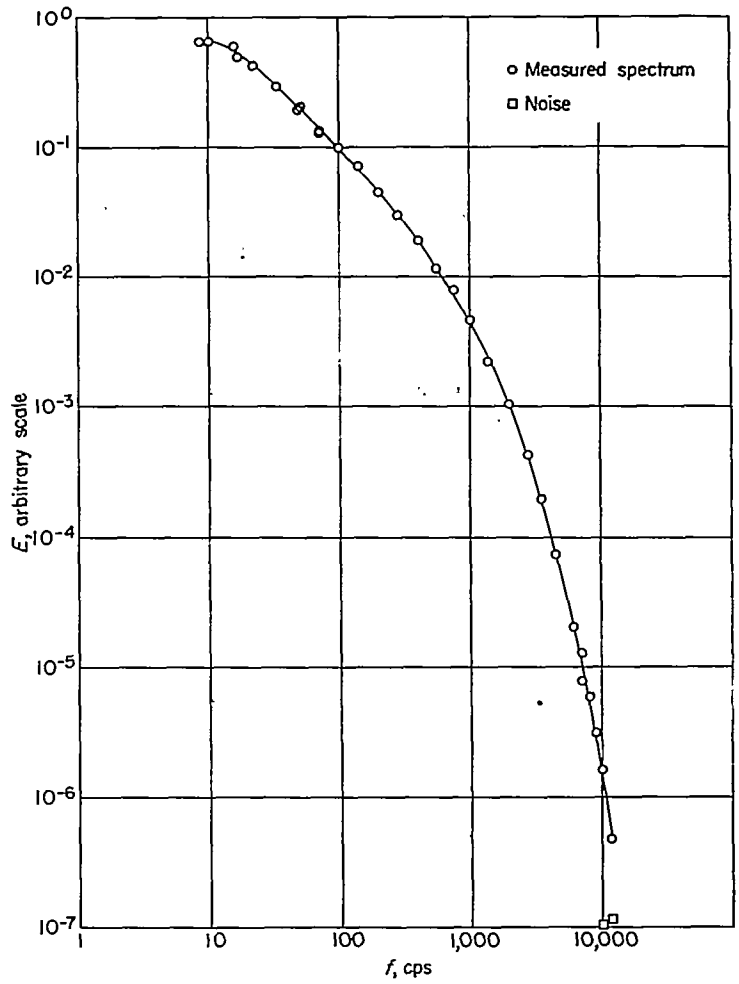

FIGURE 47.—Energy spectrum of turbulent velocity fluctuations in low-speed boundary layer. Free-stream velocity U_0=50 feet per second; boundary-layer thickness, 3 inches; distance of probe from surface, 0.15 inch; local mean velocity U/U_0=0.63; turbulence level in terms of free-stream velocity U'/U_0, 0.078.

but it rises with frequency when compensated.

The noise readings are indicated at the two highest frequencies where they are still substantially lower than the signal (points close to horizontal axis). At lower frequencies the noise spectrum is practically undetectable.

THE JOHNS HOPKINS UNIVERSITY
BALTIMORE, MD., *December 13, 1951.*

REFERENCES

1. Kovásznay, L. S. G., and Törmarck, Sven I. A.: Heat Loss of Hot-Wires in Supersonic Flow. Bumblebee Rep. No. 127, The Johns Hopkins Univ., June 1950.
2. Kovásznay, Leslie S. G.: The Hot-Wire Anemometer in Supersonic Flow. Jour. Aero. Sci., vol. 17, no. 9, Sept. 1950, pp. 565–572, 584.
3. Kovásznay, Leslie S. G.: Turbulence in Supersonic Flow. Jour. Aero. Sci., vol. 20, no. 10, Oct. 1953, pp. 657–674, 682.
4. Dryden, Hugh L., Schubauer, G. B., Mock, W. C., Jr., and Skramstad, H. K.: Measurements of Intensity and Scale of Wind-

Tunnel Turbulence and Their Relation to the Critical Reynolds Number of Spheres. NACA Rep. 581, 1937.
5. Uberoi, Mahinder S., and Kovásznay, Leslie S. G.: Influence of Resolving Power on Measurement of Correlations and Spectra of Random Fields. Tech. Rep. No. 30, Project Squid, The Johns Hopkins Univ.
6. Uberoi, Mahinder S., and Kovásznay, Leslie S. G.: On Mapping and Measurement of Random Fields. Quart. Appl. Math., vol. X, no. 4, Jan. 1953, pp. 375–393.
7. King, Louis Vessot: On the Convection of Heat From Small Cylinders in a Stream of Fluid: Determination of the Convection Constants of Small Platinum Wires With Applications to Hot-Wire Anemometry. Phil. Trans. Roy. Soc. (London), ser. A, vol. 214, Nov. 12, 1914, pp. 373–432.
8. Dryden, H. L., and Kuethe, A. M.: The Measurement of Fluctuations of Air Speed by the Hot-Wire Anemometer. NACA Rep. 320, 1929.
9. Lowell, Herman H.: Design and Applications of Hot-Wire Anemometers for Steady-State Measurements at Transonic and Supersonic Airspeeds. NACA TN 2117, 1950.
10. Spangenberg, W. G.: Heat-Loss Characteristics of Hot-Wire Anemometers at Various Densities in Transonic and Supersonic Flow. NACA TN 3381, 1954.
11. Kovásznay, Laszlo: Calibration and Measurement in Turbulence Research by the Hot-Wire Method. NACA TM 1130, 1947.
12. Townsend, A. A.: The Measurement of Double and Triple Correlation Derivatives in Isotropic Turbulence. Proc. Cambridge Phil. Soc., vol. 43, pt. 4, Oct. 1947, pp. 560–570.
13. Ossofsky, Eli: Constant Temperature Operation of the Hot-Wire Anemometer at High Frequency. Rev. Sci. Instr., vol. 19, no. 12, Dec. 1948, pp. 881–889.
14. Kovásznay, Leslie S. G.: Simple Analysis of the Constant Temperature Feedback Hot-Wire Anemometer. CM–478, Dept. Aero., The Johns Hopkins Univ., June 1, 1948.

TABLE 1.—PARTS LIST FOR CONNECTORS OF ELECTRICAL CIRCUITS

Symbol	Description	Manufacturer	From	To	Signal
P1	AN-3102A-12S-3P&S / AN-3106A-12S-3P&S	Am. Phenolic Corp	Square-wave generator	Control unit	10 v
P2	See P1		Control unit	Calibration unit	0–1 v d. c.
P3A	AN-3102A-14S-9P&S / AN-3106A-14S-9P&S	Am. Phenolic Corp	Filament supply	Control unit	300 v d. c.
P3B	See P3A		Plate supply	Control unit	220 v d. c.
P4	See P1		Control unit	Calibration unit	0–1 v d. c.
P5	AN-3102A-14S-1P&S / AN-3106A-14S-1P&S	Am. Phenolic Corp	Control unit	Compensating amplifier	0–100 mv a. c. (hot-wire signal)
P6	See P5		Calibration unit	Control unit	0–90 mv a. c.
P7	Binding posts		Hot-wire probe	Control unit	0–300 ma d. c., 0–100 mv a. c.
P8	See P5		Compensating amplifier	Service unit	0–5 v a. c., 40 v d. c. (output signal)
P9	6-140	Cinch Mfg. Corp., Howard B. Jones Div.	Power supply	Compensating amplifier	300 v d. c., 117 v a. c.
P10	See P1		Sine-wave generator	Calibration unit	0–10 v a. c.
P11	Binding posts			Control unit	Access terminal to d-c potentiometer
P12	See P5		Service unit	Oscilloscope or wave analyser.	High-impedance output
P13	See P5		Service unit	Power unit	Impedance matched output
P14	Binding posts		Power unit	Ratiometer	0–1.5 v d. c.
P15	See P1		Power unit		0–1.5 v d. c. and a. c. (square output)
P16	See P3A			Power unit	117 v a. c.
P17	See P1		Power unit	Oscilloscope	Input-signal monitor